© 2017. Published by The Company of Biologists Ltd | Development (2017) 144, 767-777 doi:10.1242/dev.146100

Severe pre-eclampsia is associated with alterations in cytotrophoblasts of the smooth chorion

Tamara Garrido-Gomez[1,2,3,4], Katherine Ona[1,2], Mirhan Kapidzic[1,2], Matthew Gormley[1,2], Carlos Simón[3,4,5], Olga Genbacev[1,2] and Susan J. Fisher[1,2,6,7,*]

ABSTRACT

Pre-eclampsia (PE), which affects ~8% of first pregnancies, is associated with faulty placentation. Extravillous cytotrophoblasts (CTBs) fail to differentiate properly, contributing to shallow uterine invasion and deficient spiral artery remodeling. We studied the effects of severe PE (sPE) on the smooth chorion portion of the fetal membranes. The results showed a significant expansion of the CTB layer. The cells displayed enhanced expression of stage-specific antigens that extravillous CTBs normally upregulate as they exit the placenta. Transcriptomics revealed the dysregulated expression of many genes (e.g. placental proteins, markers of oxidative stress). We confirmed an sPE-related increase in production of PAPPA1, which releases IGF1 from its binding protein. IGF1 enhanced proliferation of smooth chorion CTBs, a possible explanation for expansion of this layer, which may partially compensate for the placental deficits.

KEY WORDS: Pre-eclampsia, Preterm birth, Chorion, Cytotrophoblast, PAPPA1, Human

INTRODUCTION

Human placentation involves a remarkable series of interactions between embryonic/fetal trophoblasts and maternal cells (Burton and Jauniaux, 2015; Maltepe and Fisher, 2015). In most of the villous placenta (chorion frondosum), cytotrophoblasts (CTBs) fuse to form a multinucleated epithelium that is perfused with maternal blood. Thus, they are ideally positioned to transport growth-promoting substances to the embryo/fetus, which they exchange for spent material. However, near the uterine wall, CTBs adopt a different fate. They leave the villi, forming columns of mononuclear cells, which anchor the placenta to the uterus, which they subsequently invade. The intricacies of CTB interactions with maternal cells that reside within the uterine wall involve many layers of cell-cell interactions. Within the interstitial compartment, they mingle with decidual and immune cells, eventually penetrating as far as the inner third of the myometrium. Invasive CTBs also remodel the uterine vasculature. They open up the spiral arteries, enabling placental perfusion, which substantially increases as they line and enlarge these vessels. They also breach uterine veins, which establishes venous return.

Defects in placentation are mechanistically related to several of the most clinically significant pregnancy complications. The CTB differentiation pathway that leads to uterine invasion appears to be particularly vulnerable, perhaps due to the unusual cell-cell interactions that occur, its explosive nature and the exceptional plasticity of the cells. Defects in this CTB subpopulation are associated with several pregnancy complications, but most consistently, pre-eclampsia (PE). In this syndrome, CTB invasion of the interstitial compartment is frequently shallow (Brosens et al., 1970). Similar patterns are observed during placentation in nonhuman primates, including the baboon and macaque (Enders et al., 2001), suggesting that this might not be a major determinant. Instead, failed vascular invasion is thought to be the crucial defect, a theory that is bolstered by the fact that restricting blood flow to the uterus and placenta creates some of the clinical signs of PE in animal models (Abitbol et al., 1977; Granger et al., 2006). Compared with normal pregnancy, many fewer spiral arteries show evidence of CTB remodeling, and the process is often less robust in those that do. Accordingly, they retain fundamental aspects of pre-pregnancy anatomy, which precludes carrying the amount of blood that the placenta needs to develop and function properly. Currently, development of PE is thought to involve a two-stage process in which abnormal placentation, the instigator, leads to a maternal inflammatory response (Redman and Sargent, 2005).

In comparison with the trophoblast components of the chorion frondosum, the CTBs that reside in the chorion laeve or smooth chorion (sch) have received little attention. schCTBs comprise the outer surface of the fetal membranes, external to the amnion and its stroma, which is shared with the smooth chorion. Here, this subpopulation of CTBs forms a second interface with the decidua, which they appear to invade, albeit more superficially than CTBs that emigrate from the chorion frondosum, which are found throughout the decidua basalis and inner third of the muscular portion of the uterine wall. Additionally, schCTBs do not invade uterine blood vessels. Thus, vascular remodeling is confined to the decidua basalis. Very little is known about the functions of these cells. A recent review suggested that they might play an active role, via their invasive activity, in fusion of the fetal membranes with the parietal decidua (Genbacev et al., 2015). This CTB subpopulation could also be involved in rupture of the fetal membranes at birth. In this regard, inducible nitric oxide synthase and cyclooxygenase-2 (also known as prostaglandin-endoperoxide synthase 2) contribute to the induction of apoptosis in these cells (Yuan et al., 2006, 2009), as does an imbalance in the production and elimination of reactive

[1]Center for Reproductive Sciences, University of California San Francisco, San Francisco, CA 94143, USA. [2]Department of Obstetrics, Gynecology, and Reproductive Sciences, University of California San Francisco, San Francisco, CA 94143, USA. [3]Fundación Instituto Valenciano de Infertilidad (FIVI), Instituto Universitario IVI, INCLIVA, Biomedical Research Institute, Valencia University, Valencia, 46010, Spain. [4]Fundación Igenomix, Valencia, 46980, Spain. [5]Department of Obstetrics and Gynecology, School of Medicine, Stanford University, CA 94305, USA. [6]The Eli & Edythe Broad Center for Regeneration Medicine and Stem Cell Research, University of California San Francisco, San Francisco, CA 94143, USA. [7]Department of Anatomy, University of California San Francisco, San Francisco, CA 94143, USA.

*Author for correspondence (sfisher@cgl.ucsf.edu)

S.J.F., 0000-0001-7745-4850

Received 3 November 2016; Accepted 30 December 2016

Development (2017) 144, 767-777 doi:10.1242/dev.146100

oxygen species (Yuan et al., 2008). Here, we tested the hypothesis that the defects in the chorion frondosum that are associated with PE extend to the smooth chorion. Surprisingly, the results showed changes consistent with the novel concept that, in this syndrome, the later population of CTBs expands, which could compensate for anatomical and functional deficits in the placenta.

RESULTS

The CTB layer of the smooth chorion expands in sPE

In cases in which the fetal membranes were intact, Hematoxylin and Eosin (H&E) staining revealed a single layer of amniotic epithelial (AMNION EP) cells that was connected to the smooth chorion via a shared stromal compartment. The outer CTB portion was in direct contact with the decidua parietalis. During early second trimester of normal pregnancy, the smooth chorion contained numerous villous remnants, termed ghost villi (GV) (Fig. 1A). The CTB layer (schCTB) was ill-defined and in some areas the fetal cells intermingled with the decidua. As gestation proceeded, the number of GV declined precipitously (Fig. 1B). By the end of the second trimester, few-to-none of these structures were visible. The schCTB layer had a more condensed appearance, and there was a defined border between the fetal cells and the decidua (Fig. 1C). It is likely that the observed changes are secondary to several factors. One is the loss of a direct blood supply. Another is establishment of the utero-placental circulation at the end of the first trimester of pregnancy, which results in a significant rise in oxygen tension. Placental perfusion is most robust at the center, creating oxidative stress at the margins (Burton et al., 2010).

We also analyzed tissue sections of the intact fetal membranes from five sPE and five preterm labor cases with no signs of infection (non-infected preterm birth, nPTB) (25-34 weeks). The maternal and neonatal characteristics are summarized in Table S1. Higher power magnifications of the photomicrographs revealed

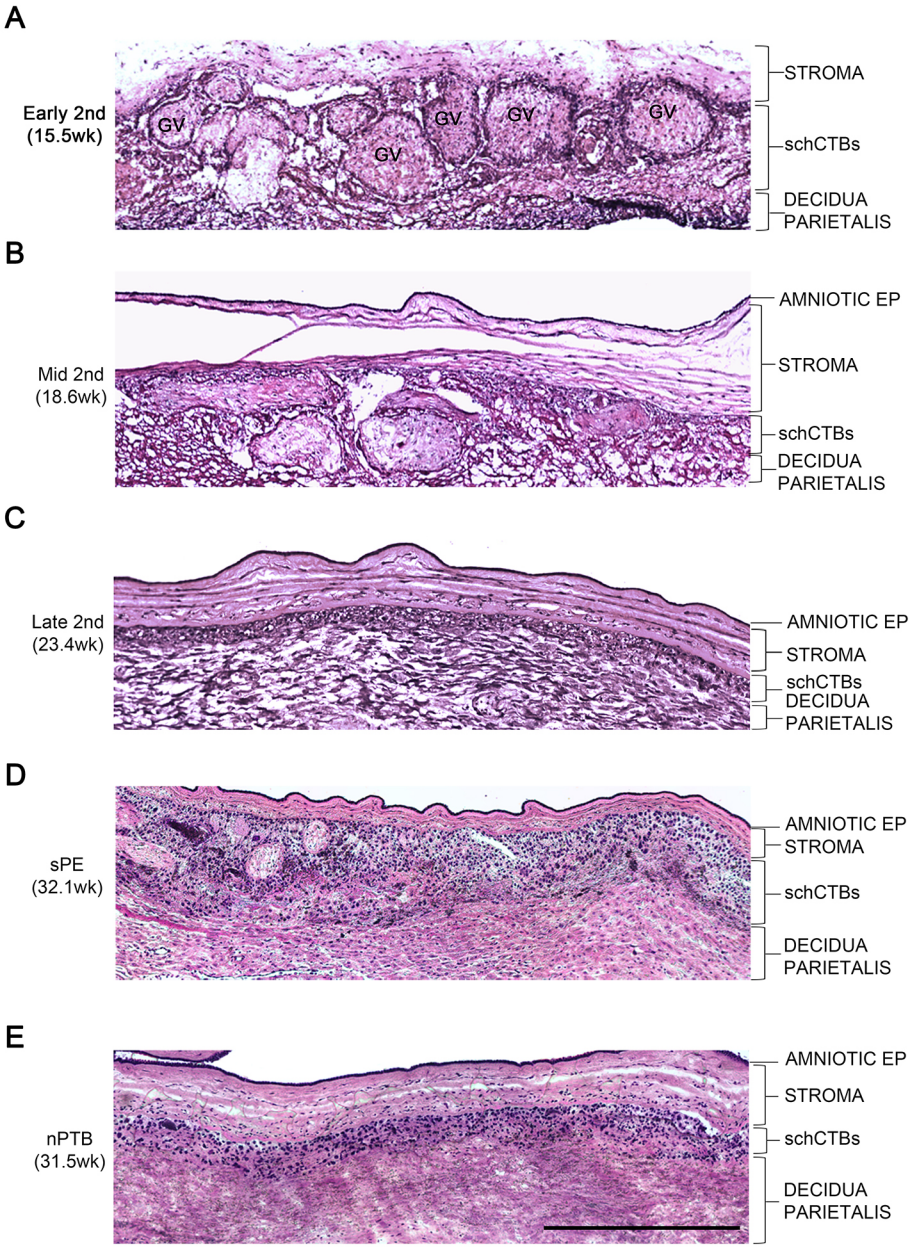

Fig. 1. The CTB layer of the smooth chorion expands in sPE. Tissue sections from samples of this region, during the second trimester of normal pregnancy, and specimens from non-infected preterm birth (nPTB) and severe pre-eclampsia (sPE) were stained with H&E. (A) During early second trimester, the smooth chorion contained numerous ghost villi (GV). The CTB layer (schCTB) was disorganized, intermingling with the decidua. (B) As gestation proceeded, fewer GV were observed. (C) By the end of the second trimester, few (to no) GV were visible. The schCTBs became a defined layer adjacent to the decidua. (D) In sPE, the morphology of the smooth chorion resembled that of samples from the first half of the second trimester (compare A, B and D). (E) In contrast, the morphology of this region in nPTB was comparable to that of late second trimester specimens (compare C and E). In some cases, the stroma was more loosely organized than in the equivalent layer from sPE cases (compare D and E). *n*=5/group. EP, epithelium. Scale bar: 500 µm.

Development (2017) 144, 767-777 doi:10.1242/dev.146100

greater detail (Fig. 1) and lower power magnifications enabled assessment of nearly the entire membrane (Fig. S1). There were no notable differences between the appearances of the amniotic epithelium in the two pregnancy complications. In nPTB, some areas of the stroma appeared to be more loosely organized than in the equivalent layer from sPE cases (compare Fig. 1D,E). The major finding was the morphological resemblance of the smooth chorion from sPE cases to early and mid-second trimester samples (compare Fig. 1A,B,D). In addition to an expansion of the schCTB population, the layer was less organized and numerous GV were evident, which appeared with lower frequency in samples from nPTB cases that had morphological features of late second trimester samples (compare Fig. 1C,E). In some nPTB samples, the adjacent decidual layer was also somewhat disorganized. Thus, in sPE, the schCTB layer of the fetal membranes retained morphological features of the earlier gestation samples.

To confirm and extend these findings, we double immunostained fetal membrane samples with anti-cytokeratin (CK), which labels CTBs and amniocytes, and anti-vimentin, which reacts with cells of the stromal layer of the membranes and the decidua (Fig. 2). As previously reported, amniocytes in some samples also gave a vimentin signal (Behzad et al., 1995). The results confirmed the

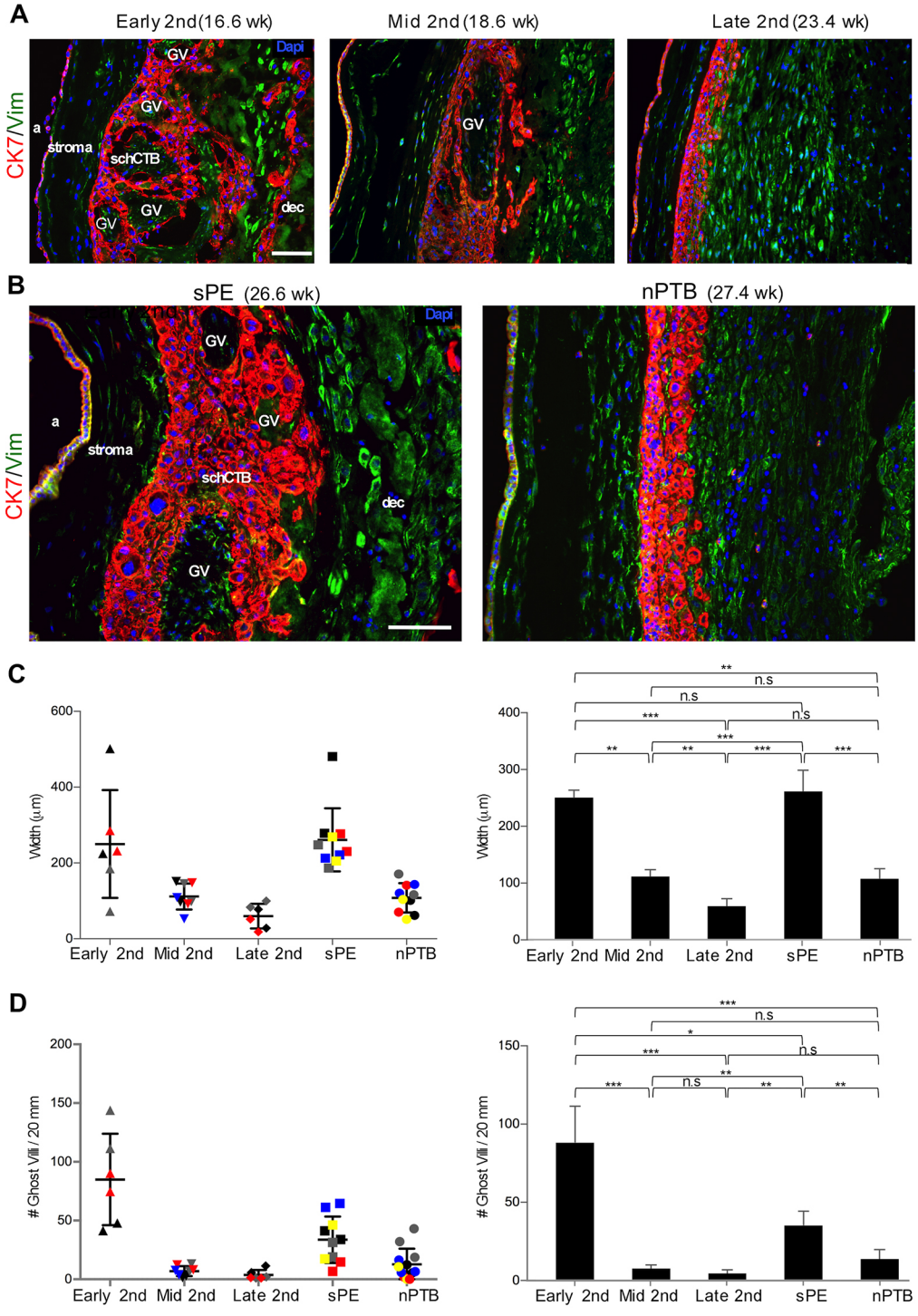

Fig. 2. Immunolocalization of cytokeratin confirmed expansion of the schCTB layer and retention of GV in sPE. The samples were double immunostained. Anti-cytokeratin (CK7) labeled CTBs and amniotic epithelial cells. Anti-vimentin (Vim) reacted with the decidua, the stromal layer of the fetal membranes and, in some samples, the amniotic epithelium. (A) The results confirmed intermixing of the schCTB layer and decidua in early second trimester samples, the reduction in GV as pregnancy advanced, and the reorganization into a defined layer by late second trimester. (B) Cytokeratin immunolocalization also confirmed the morphological differences between the sPE and nPTB samples that were observed in the H&E-stained specimens (see Fig. 1D,E). (C) Quantification revealed an approximate 80% decrease in the width of the schCTB layer during the second trimester interval examined. The width of the schCTB layer in sPE was comparable to that of early second trimester specimens and nPTB samples were similar to the late second trimester samples. (D) Quantification revealed a dramatic reduction of GV during the second trimester of normal pregnancy. In sPE, the schCTB layer contained fewer GV than the early gestation samples, but more than in nPTB. *n*=5/group. In C and D, two areas of the same sample (individual samples denoted by different colors and symbols) were analyzed. **P*<0.05; ***P*<0.01; ****P*<0.001; n.s., not significant. a, amnion; dec, decidua. Scale bars: 100 µm.

Development (2017) 144, 767-777 doi:10.1242/dev.146100

intermixing of the schCTB layer and decidua in early second trimester samples and the reduction in GV as pregnancy neared the third trimester (Fig. 2A). CK immunolocalization confirmed the morphological differences between the sPE and nPTB samples (Fig. 2B) that were observed in the H&E-stained specimens (Fig. 1D,E). Next, we quantified two major features of the schCTB layer during the second trimester of normal pregnancy and in sPE versus nPTB. On average there was an approximate 80% decrease in the width of this layer during the second trimester (Fig. 2C). Measuring this parameter in sPE samples showed that the width of the schCTB layer was comparable to that of early second trimester specimens. In this regard, nPTB samples were similar to the mid and late second trimester specimens. As to GV, there was a dramatic reduction during the second trimester of normal pregnancy (Fig. 2D). In sPE, the schCTB layer contained approximately twice the number of GV compared with the nPTB samples, and the frequency was higher than in the mid and late second trimester specimens. Together, these results suggested that the schCTB layer of the fetal membranes in sPE retained the morphological features of the early second trimester samples. In nPTB, this layer had the morphology of late second trimester samples from normal pregnancy.

sPE is associated with increased expression in schCTBs of a combination of villous and extravillous CTB stage-specific antigens

Next, we examined the expression of antigens that are misregulated in the basal plate region in pregnancies that are complicated by sPE. Specifically, invasive CTBs downregulate the expression of HLA-G (Lim et al., 1997), misexpress several integrins (Zhou et al., 1993) and upregulate E-cadherin (cadherin 1) (Zhou et al., 1997). These changes are associated with a failure of CTBs within the uterine wall to express vascular-type antigens (Zhou et al., 1997).

As to the smooth chorion in the second trimester of normal pregnancy, a subset of CTBs toward the decidual interface reacted with anti-HLA-G, anti-integrin α4 and anti-E-cadherin (Fig. 3A-C). In general, the number of cells that immunostained was reduced

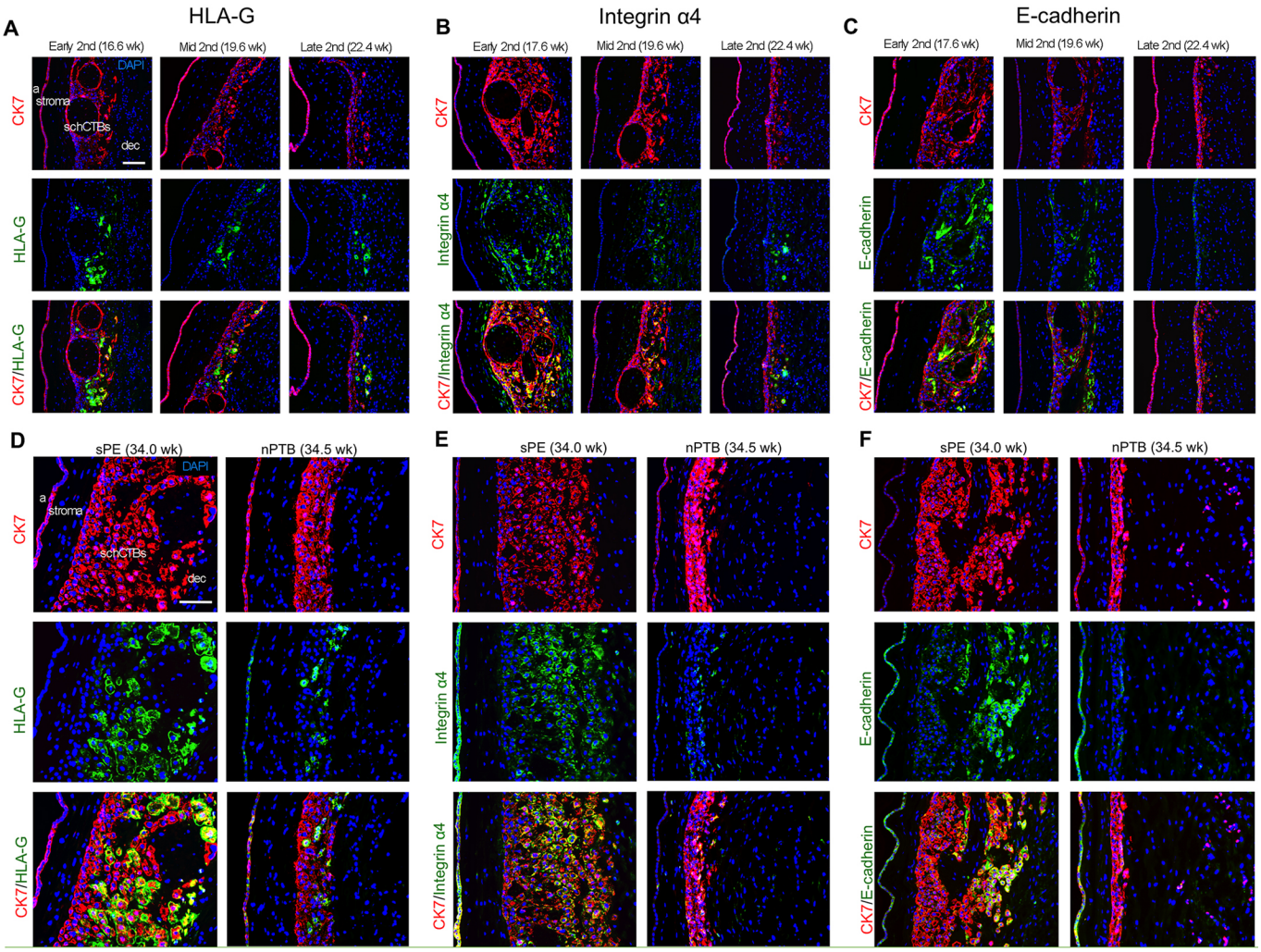

Fig. 3. In sPE, a subpopulation of schCTBs showed strong staining for stage-specific antigens, which invasive/extravillous CTBs upregulate as they emigrate from the placenta. (A) In early second trimester of normal pregnancy, a subset of CTBs throughout the smooth chorion reacted with anti-HLA-G. By late second trimester, fewer cells immunostained. (B) The same general pattern was observed for anti-integrin α4 immunoreactivity. (C) Numerous schCTBs reacted with anti-E-cadherin in early second trimester. This subpopulation was largely absent in samples from the late second trimester of normal pregnancy. (D) Compared with second trimester and nPTB samples, the proportion of cells that reacted with anti-HLA-G was higher in sPE. (E,F) Expression of integrin α4 (E) and E-cadherin (F) was upregulated in sPE compared with nPTB. The images are representative of the analysis of a minimum of three sections from different samples (n=5). a, amnion; dec, decidua. Scale bars: 100 µm.

Development (2017) 144, 767-777 doi:10.1242/dev.146100

(HLA-G and integrin α4) or nearly absent (E-cadherin) by late second trimester. At this stage, immunopositive cells were most often found at the decidual boundary. We failed to detect expression in schCTBs of vascular-type molecules that extravillous CTBs express within the uterine wall and blood vessels – PECAM (platelet and endothelial cell adhesion molecule), VCAM (vascular cell adhesion molecule), VE-cadherin (cadherin 5) and VEGFA (vascular endothelial growth factor A) (data not shown). Thus, this subpopulation of CTBs has similarities with and differences from invasive extravillous cells.

In comparison to the second trimester of normal pregnancy, the proportion of cells that reacted with an antibody that specifically recognized HLA-G was higher in sPE (Fig. 3D). The fraction of cells that expressed this antigen in nPTB was similar to that observed in the late second trimester samples. With regard to the integrin α4 and E-cadherin expression patterns in the pregnancy complications that we studied, the major finding was upregulated expression in sPE compared with nPTB (Fig. 3E,F). For the three antigens whose expression we studied, the immunopositive cells were oriented toward the decidua rather than the amnion. As in the second trimester samples from normal pregnancies, no expression of the vascular-type antigens we assayed was detected in the pregnancy complication groups (data not shown). Together, these results suggested that schCTBs in sPE versus nPTB have more widespread expression of the stage-specific antigens that the extravillous subpopulation normally upregulate in columns and the superficial decidua.

During the second trimester of normal pregnancy isolated schCTBs are more invasive than villous CTBs

In these experiments, we quantified invasion by using a Matrigel penetration assay in which CTBs are plated on matrix-coated filters and the number of cells that reach the underside are counted. First, we compared the behavior of schCTBs and their villous (v) counterparts from the same donors. During the second trimester of normal pregnancy, CTBs from the smooth chorion were more invasive than vCTBs at all the gestational ages that were examined (Fig. 4A,B). The invasiveness of CTBs isolated from both compartments decreased during the second trimester.

sPE is associated with increased schCTB invasiveness compared with nPTB

Next, we investigated whether the morphological and antigenic alterations that were observed in sPE were accompanied by functional changes. The maternal and infant characteristics of the samples that went into this analysis are included in Table S1. In sPE, schCTBs were once again more invasive than vCTBs and as compared with schCTBs and vCTBs in nPTB (Fig. 4A,B). Although variability impacted the statistical significance, CTBs from the sPE smooth chorion tended to mimic the invasion levels of the second trimester samples. In contrast, comparable levels of invasion were observed in the later second trimester, sPE and nPTB vCTB samples. Thus, these data suggested either an autocrine or a paracrine braking mechanism that restrains schCTB invasion *in vivo* and that sPE is associated with increased invasiveness of these cells, perhaps overcoming this barrier. We hypothesize that the sPE-related changes in the schCTBs subpopulation are, at least in part, a compensatory mechanism for functional deficits in vCTBs, particularly with regard to differentiation along the extravillous pathway.

sPE impacts schCTB gene expression

To gain a better understanding of the molecular mechanisms behind the observed schCTB alterations in sPE, we used a laser capture microdissection approach to isolate this population of cells from the fetal membranes of sPE and nPTB pregnancies (n=4/group). The maternal and neonatal characteristics associated with the samples used for microarray analysis are summarized in Table S2. There were no differences in maternal characteristics other than elevated blood pressure and proteinuria in the sPE group. Neonatal weights were also lower in this group.

Microarray analyses enabled a global comparison of the cells' gene expression patterns in the two conditions. In sPE schCTBs,

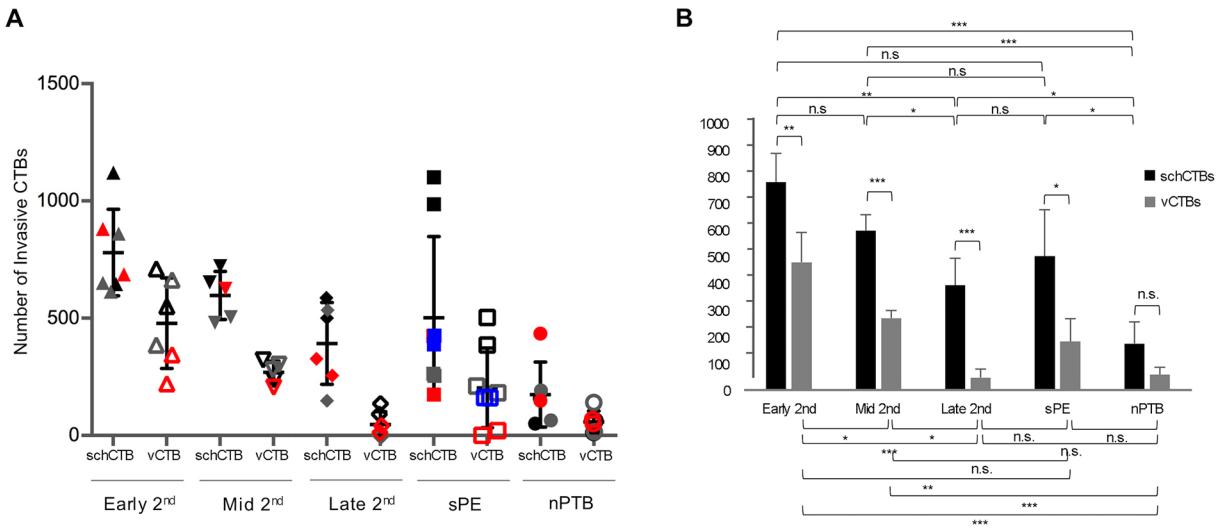

Fig. 4. Quantification of cytotrophoblast invasion: smooth chorion versus chorionic villi and sPE versus nPTB. (A,B) Invasion was assayed using a Matrigel penetration assay in which cells are plated on Matrigel-coated filters and the number of cells that reached the filter underside were counted. The overall approach was to compare the behavior of cytotrophoblasts isolated from the two compartments. With the exception of nPTB samples, cytotrophoblasts from the smooth chorion (schCTB) were more invasive than their villous counterparts (vCTBs). During the second trimester of normal pregnancy, the invasiveness of CTBs isolated from both compartments decreased with advancing gestational age. sPE was associated with increased invasiveness of schCTBs compared with the comparable population of cells isolated from the placentas of nPTB cases such that the levels were similar to second trimester cells. n=3-4 CTB preparations isolated from different placentas per experimental group (denoted by colors). Samples were assayed in duplicate. *P<0.05, **P<0.01, ***P<0.001; n.s., not significant.

Development (2017) 144, 767-777 doi:10.1242/dev.146100

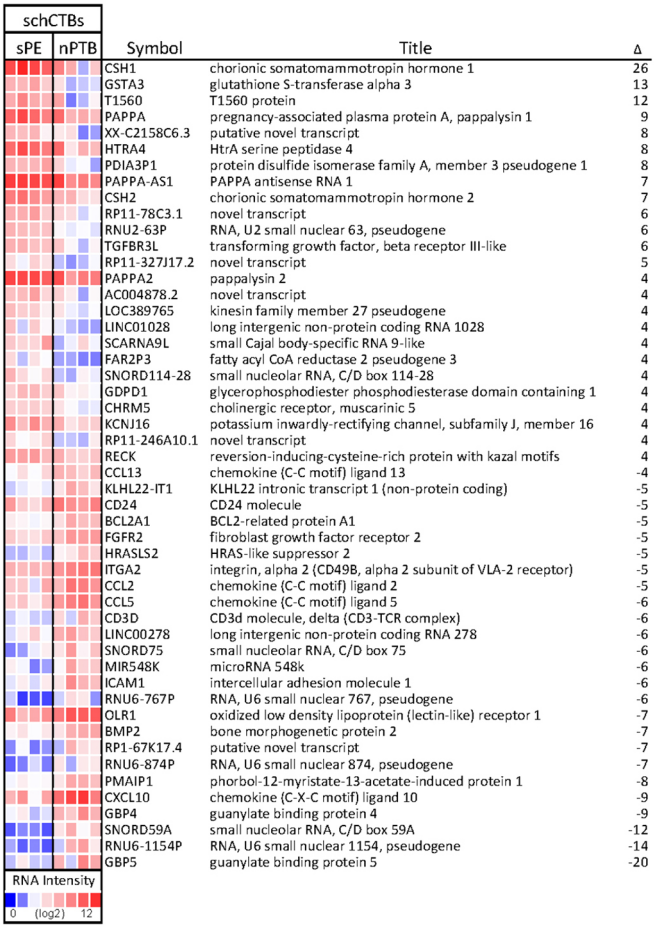

Fig. 5. Global transcriptional profiling of cytotrophoblasts from the smooth chorion revealed sPE-associated aberrations in gene expression. The cells were isolated by laser capture microdissection. Then RNA was prepared and gene expression analyzed using an Affymetrix microarray platform. The relative expression levels of the 50 most highly differentially expressed genes (severe pre-eclampsia, sPE) versus non-infected preterm birth (nPTB) are shown as a heat map (red, upregulated; blue, downregulated). The fold changes are shown on the right (Δ). *n*=4 sPE samples and 4 nPTB samples. T1560 (LINC01602); KLHL22-IT1 (RNY1P9); LOC389765 (gene kinesin family member 27 pseudogene RP11-213G2.3).

116 genes were upregulated (2-fold and higher) and 133 genes were downregulated (2-fold and higher) compared with nPTB (Fig. 5, 50 most highly differentially expressed; Fig. S2, complete list). The most highly upregulated genes were *CSH1* (also known as *HPL*; 26-fold), glutathione S-transferase alpha 3 (*GSTA3*; 13-fold) and *PAPPA1* (*PAPPA*; 9-fold). Two related molecules, PAPPA antisense RNA 1 and *PAPPA2*, were also upregulated (7-fold and 4-fold, respectively). Another placental lactogen, chorionic somatomammotropin hormone 2, was upregulated 7-fold. Thus, several placenta-specific proteins were modulated in sPE as was *GSTA3*, which functions in hormone production and detoxification. Upregulation of *TGFBR3L* (6-fold), which binds TGFβ family members via its heparan sulfate chains, suggests the possibility of enhanced growth factors signaling in sPE.

Conversely, we found upregulation, in nPTB, of immune molecules, guanylate binding proteins 5 and 4 (GBPs; 20-fold and 9-fold, respectively), *CXCL10* (9-fold), *ICAM1* (6-fold), *CD3D* (6-fold), *CCL5* (6-fold), *CCL2* (5-fold), *CD24* (5-fold) and *CCL13* (4-fold). As a group they have many interesting immune-related functions. GBP4 dampens interferon-induced viral responses (Hu et al., 2011) and GBP5 is an interferon-inducible inhibitor of viral infectivity including HIV (Krapp et al., 2016). These chemokine-related and adhesion molecules promote chemotaxis of monocytes/macrophages, T cells, NK cells and dendritic cells; T cell adhesion to endothelial cells; and angiogenesis. ICAM strengthens intercellular adhesion, and CD3D is a component of the T-cell receptor. These data suggested that inflammation and immune processes were activated in nPTB even when there were no clinical signs of overt infection. Other genes that were downregulated in schCTBs from sPE compared with nPTB (e.g. *BMP2*, 7-fold; *FGFR2*, 5-fold) might be related to aberrations in growth factor signaling.

We also compared gene expression of schCTBs in sPE and nPTB with the equivalent population of cells that were laser captured from fetal membranes, which were obtained during the second trimester of normal pregnancy (Fig. S3A). In general, the gene expression patterns of the nPTB samples were more similar to the second trimester schCTBs than were those of the equivalent sPE population. Hierarchical clustering failed to entirely separate the second trimester and nPTB samples. In contrast, the equivalent cells from sPE cases clustered together (Fig. S3B). Thus, although the schCTB layer of the smooth chorion had morphological features of early second trimester samples, global transcriptional profiling showed major differences at a molecular level.

In comparison with normal second trimester schCTBs, the mostly highly upregulated genes in sPE samples (Fig. S4) were *MT1H* (23-fold) and *MT1G* (13-fold), providing evidence of oxidative stress, which was consistent with the vascular constriction that was observed in the adjacent decidual compartment (data not shown). Corneodesmosin, which is related to cornification of epithelial layers, was also highly upregulated (10-fold) in sPE. Whether or not this is functionally related to the expansion of the schCTB layer in these cases remains to be determined. *PAPPA1* and *GSTA3* expression was also higher than in normal second trimester samples (8-fold and 4-fold, respectively). With regard to genes for which expression was downregulated in sPE versus second trimester samples, several chemokine family members were in this category, suggesting that their upregulation in nPTB might not be related to this condition, e.g. *CD24* (10-fold), *CXCL10* (6-fold) and *CCL2* (6-fold). Interestingly, expression of *NPPB* (11-fold), which acts to decrease blood pressure, was also reduced in sPE. Thus, immunolocalization of stage-specific antigens, invasion assays and gene expression data pointed to schCTB dysregulation in sPE.

We also compared gene expression of schCTBs in nPTB versus the equivalent population of cells that were laser captured from fetal membranes obtained during the second trimester of normal pregnancy (Fig. S5). The most highly upregulated genes included a serine peptidase inhibitor (*SPINK1*; 12-fold), *HLA-DR* (12-fold) and *BMP2* (7-fold). The genes downregulated to the greatest extent included histone *H2AM* (*HIST1H2AM*; 11-fold) and *CGA* (8-fold). Overall, small nuclear RNAs were highly differentially expressed in this dataset.

Validation of the differentially expressed genes at the protein level

Next, we investigated whether the highly upregulated mRNAs were accompanied by an equally dramatic increase in expression at the protein level. Accordingly, we immunolocalized CSH1 (HPL) in tissue sections of the fetal membranes from sPE and nPTB cases (*n*=4/group; Table S1). Little immunoreactivity was detected in the CTB layer of the smooth chorion from pregnancies that were

Development (2017) 144, 767-777 doi:10.1242/dev.146100

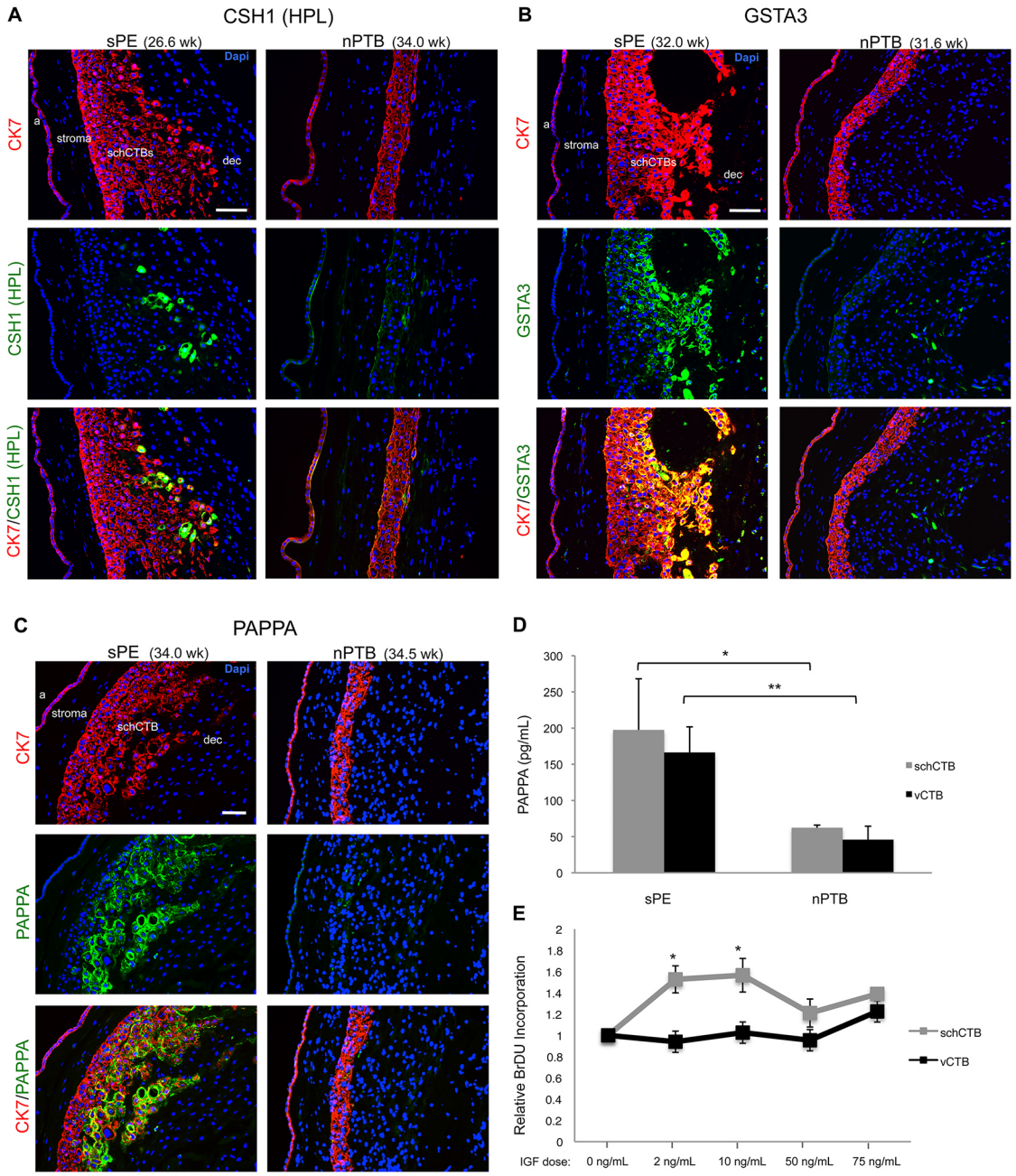

Fig. 6. Confirmation of the microarray results: protein level and functional data. CSH1, GSTA3 and PAPPA1 immunoreactivity corroborated differential expression at the RNA level. The identity of cytotrophoblasts in the smooth chorion (schCTBs) was confirmed by cytokeratin (CK) expression. (A) Little to no signal for CSH1 was detected in cases of non-infected preterm birth (nPTB). In contrast, a subset of schCTBs interspersed among the immunonegative cells stained strongly with an antibody that recognized this molecule. (B) In sPE, the same pattern of differential expression was observed for GSTA3 except that immunoreactivity was more widespread among the schCTBs and the signal was associated with cells that were adjacent to the decidua parietalis. (C) Immunolocalization of PAPPA in the fetal membranes showed high CTB-associated immunoreactivity in sPE compared with largely background staining in nPTB. The images are representative of the analysis of a minimum of three sections from different areas of smooth chorion biopsies for each case (n=4/group). Cytokeratin (CK7) expression confirmed trophoblast identity and DAPI staining enabled visualization of nuclei. a, amnion; dec, decidua. Scale bars: 100 µm. (D) ELISA quantification of CTB PAPPA1 secretion into the culture medium. In sPE, vCTB and schCTB release of PAPPA1 significantly increased compared with the same subpopulations of cells in nPTB. n=3/group. (E) Isolated schCTBs and vCTBs (n=3 second trimester samples/group) were cultured in the presence of exogenous IGF1. Compared with baseline (no addition), IGF1 (2 and 10 ng) increased BrDU incorporation by schCTB, but not vCTBs. *P<0.05; **P<0.01.

complicated by nPTB. In contrast, sPE was associated with strong anti-CSH1 immunoreactivity in a subset of CTBs that tended to be located near the decidual junction (Fig. 6A). Essentially the same result was obtained for GSTA3. However, a greater proportion of the CTB population was immunopositive (Fig. 6B).

PAPPA1-stimulated proliferation of schCTBs

Finally, we were interested in determining whether any of the upregulated molecules could be functionally related to the observed sPE-associated increase in the number of CTBs that resided within the smooth chorion. Given its ability to cleave IGFBP4 and -5,

Development (2017) 144, 767-777 doi:10.1242/dev.146100

releasing the bound IGF1 (Gaidamauskas et al., 2013), we were interested in the expression and function of PAPPA1. Immunolocalization of this antigen in the fetal membranes showed high CTB-associated immunoreactivity in sPE compared with largely background staining in nPTB (Fig. 6C). Additionally, we assayed CTB secretion of PAPPA1 into the conditioned medium. In sPE, villous and schCTB release of PAPPA1 significantly increased compared with the same populations in nPTB (Fig. 6D). Thus, this pregnancy complication is associated with highly upregulated production and secretion of PAPPA1 by CTBs of the placenta and smooth chorion.

To determine the consequences, we isolated schCTBs and vCTBs (n=3 second trimester samples/group) and cultured them in the presence of exogenous IGF1. Compared with base-line (no addition), IGF1 (2 and 10 ng) increased bromodeoxyuridine (BrDU) incorporation by schCTB, but not vCTBs (Fig. 6E). Together, these data suggested that sPE-associated increases in PAPPA1 could be at least partially responsible for the observed expansion of the schCTB layer in this pregnancy complication. Alternatively, enhanced expression of PAPPA1 and its effects on CTB proliferation could be attributable to a delay or halting of differentiation such that, in sPE, the later gestation smooth chorion has features that are more typical of second trimester samples.

DISCUSSION

It has been nearly 50 years since PE was linked to malformations of the maternal-fetal interface, in particular to deficient CTB remodeling of the uterine vasculature (Brosens et al., 1970). In normal pregnancy and in PE, very little is known about the other region where CTBs interface with the decidua – the smooth chorion. We studied this portion of the fetal membranes, during the second trimester of normal pregnancy, in relationship to sPE and nPTB. At a morphological level, two major features of the smooth chorion changed in the interval between early and late second trimester. The width of the CTB layer dramatically decreased along with the number of GV. In sPE, the smooth chorion retained characteristics of the early gestation normal samples – a wide CTB layer with numerous GV that were absent in the equivalent region of the nPTB samples, which resembled the morphology of the smooth chorion in the late second trimester of normal pregnancy.

At a molecular level, schCTBs were a distinct CTB subpopulation. Initially, we examined the cells' expression of stage-specific antigens that villous CTBs modulate as they exit the chorion frondosum and invade the decidua. In line with the fact that there was no morphological evidence of uterine blood vessel invasion, the cells did not express the vascular-type cell adhesion molecules that they normally upregulate within the uterine wall, including PECAM, VCAM, VE-cadherin and VEGFA (Zhou et al., 1997). They also did not express integrin α1, which plays an important role in invasion (Damsky et al., 1994). During the second trimester of normal pregnancy, schCTB immunostained for a combination of antigens that are expressed by villous and invasive/extravillous CTBs: E-cadherin, integrin α4 and HLA-G. In general, expression of these molecules in normal pregnancy tended to be more widespread throughout the CTB layer in early second trimester samples than in later gestation when fewer cells were antibody-reactive. In this regard, HLA-G and integrin α4 expression were confined to a subset of CTBs that were in direct contact with the decidua. Thus, CTBs of the smooth chorion had an antigenic profile that resembled cells in proximal regions of columns that have initiated differentiation along the invasive pathway.

Previous studies reported similarities (e.g. EGF receptor expression; Bulmer et al., 1989) and differences (e.g. lectin staining; Lalani et al., 1987) between schCTBs and vCTBs. Additionally, production of renin (Poisner et al., 1981; Symonds et al., 1968) and its substrate, angiotensinogen (Lenz et al., 1993), is concentrated in schCTBs. Yeh et al. (1989) described two mononuclear CTB populations in the chorion laeve. The first is vacuolated cells, with a clear cytoplasm that is rich in pinocytotic vesicles and lipid droplets. They react with antibodies that recognize human placental lactogen and placental alkaline phosphatase. The role of the latter molecule in absorption led the authors to suggest that these cells might play a role in this process. The second population of cells has an eosinophilic cytoplasm, which lacked vacuoles, and they express neither antigen. Both schCTB subtypes failed to express other molecules that are characteristic of vCTBs, including prolactin, pregnancy specific beta 1 glycoprotein and hCG beta. The antigen-positive and -negative cells that we describe, which did not clearly correspond to the either of these populations, might be a mixture of the two.

The significant morphological changes that were associated with the CTB layer of the smooth chorion in sPE were accompanied by alterations in the expression of E-cadherin, integrin α4 and HLA-G. Specifically, a large proportion of the CTBs expressed these antigens compared with the same subpopulation in either the late second trimester of normal pregnancy or in nPTB. Thus, sPE is associated with morphological and molecular alterations in the CTB layer of the smooth chorion that were reminiscent of the villous immaturity involving the chorion frondosum that was noted many years ago (Hustin et al., 1984).

The gestation-related and sPE-associated differences in the CTB subpopulation of the smooth chorion suggested the possibility of functional alterations. Accordingly, we investigated this possibility by assaying their invasive ability. With regard to normal pregnancy, second trimester schCTBs were more invasive than vCTBs isolated from the same placenta. Additionally, we observed a gestational-age related decline in invasiveness. We speculate that this surprising difference may be indicative of an active role for these cells in attaching the fetal membranes to the decidua parietalis. Whether the decidua capsularis is lost in the process or fuses with rest of the decidua during this process is uncertain (Benirschke et al., 2012). The mechanisms that restrain schCTB invasion *in vivo* are unknown, but could include enhanced expression of plasminogen activator inhibitor-1 (PAI-1 or SERPIN E1) by decidual cells in this region (Floridon et al., 2000).

Using the same experimental design, we investigated the impact of sPE on the invasiveness of schCTBs versus vCTBs. Bolstering our finding that CTBs from the chorion are more invasive than their villous counterparts, we observed the same phenomenon in sPE and nPTB samples. Furthermore, schCTBs from the placentas of sPE patients were significantly more invasive than those from the placentas of women who experienced preterm birth. We speculate that this might reflect an attempt to form more extensive interactions with maternal cells perhaps for absorptive purposes. The enhanced invasiveness of schCTBs in sPE together with the expansion of this layer described above could be in response to the pathological alterations of the chorion frondosum and invasive/extravillous CTBs that are associated with this pregnancy complication.

Global transcriptional profiling revealed the gene expression patterns of schCTBs in sPE compared with nPTB (and the second trimester of normal pregnancy). Previously, we used this approach to compare vCTB gene expression in the same pregnancy complications immediately after the cells were isolated and as

Development (2017) 144, 767-777 doi:10.1242/dev.146100

they differentiated along the invasive pathway over 48 h in culture (Zhou et al., 2013). A comparison of the two datasets yielded new insights. First, the number and magnitude of changes in gene expression that were evident in the schCTB dataset were far greater than those observed for vCTBs. This finding suggested that sPE has very significant effects on the chorion laeve as well as the chorion frondosum. Second, there was no overlap in the schCTB and vCTB genes that were dysregulated in sPE and the same was true for nPTB. This result suggested that these are two very different CTB subpopulations in normal pregnancy and in their transcriptional responses to sPE and nPTB. For example, many of the PSGs were upregulated in vCTBs isolated from the placentas of sPE cases (Zhou et al., 2013). In contrast, only PSG11 was modulated (4-fold increase) in the equivalent schCTB dataset. Together, these findings suggested that schCTBs are active participants rather than passive bystanders to the placenta's role in pregnancy. In this regard it is interesting to note the geometry of the placenta and the very large surface area formed by the smooth chorion. Our results suggested the importance of considering this 'second front' where fetal and maternal cells directly interact, which, in addition to the chorion frondosum, could play an important role in governing pregnancy outcome.

As to the dysregulated expression of specific genes, *CSH1* was the most highly upregulated schCTB transcript in sPE. In vCTBs, another transcript from this locus, *GH2*, was the most highly expressed gene (Zhou et al., 2013). In contrast to both findings, analyses of placentas from sPE cases showed that transcription from the entire locus (*GH2*, *CSH1*, *CHS2* and *CSHL1*) was downregulated (Männik et al., 2012). CSH1, which is secreted into maternal blood, regulates maternal metabolic adaptation to pregnancy. Consistent with its role in promoting intrauterine growth, it is also found in the fetal circulation (Handwerger and Freemark, 2000). Our data suggested that schCTBs might be a particularly important source of the latter fraction. The *GSTA3* transcript was also highly upregulated. This enzyme, a member of the glutathione S transferase family, plays an important role in the generation of intermediate metabolites in the biosynthesis of progesterone and testosterone (Johansson and Mannervik, 2001). Its enhanced expression in sPE suggested that schCTBs upregulate steroid production. In a rat model of this pregnancy complication, treatment with 17-hydroxyprogesterone improved uterine perfusion (Amaral et al., 2015). Whether our observation is related in terms of increased *GSTA3* expression as being an attempt to upregulate blood flow to the placenta remains to be determined. Finally, schCTBs highly expressed *PAPPA1* (and *PAPPA2*) in sPE versus nPTB. This result was in accordance with previous reports of elevated levels of this proteinase in maternal serum and/or placentas from PE cases (Kramer et al., 2016). Our investigation of increased PAPPA1 production suggested an autocrine role in expansion of the schCTB layer in sPE. Also, these data might be indicative of the smooth chorion retaining features of a more immature state. Finally, this analysis highlighted genes that were upregulated in nPTB. They included *GBP4* and *-5*, which play important roles in inflammasome assembly and function (Shenoy et al., 2012; Tyrkalska et al., 2016), possible signals of the beginning of an inflammatory response despite the absence of clinical indicators.

We also compared gene expression of schCTBs in sPE and nPTB to schCTBs in the second trimester of normal pregnancy. In sPE, the highly upregulated genes included *MT1H* and *MT1G* (Fig. S4), metal-binding proteins that protect cells from oxidative stress (You et al., 2002). Thus, our results suggested that the smooth chorion is also affected by reduced uterine perfusion. We were surprised to find a strong upregulation of corneodesmosin in sPE. This molecule is the major component of desmosomes in the stratum corneum of the skin (Ishida-Yamamoto and Igawa, 2015). This raised the possibility that components of a desquamation-like process might be involved in separation of the smooth chorion from the uterus. In the skin, SPINK family members, serine proteinase inhibitors, prevent degradation of corneodesomosomes by inhibiting the actions of kallikreins. Interestingly, *SPINK1* was the most highly upregulated gene in schCTBs from nPTB versus the second trimester of normal pregnancy (Fig. S5). In the second trimester comparison, natriuretic peptide B was the most downregulated gene in sPE. Deletion in mice results in impaired cardiac remodeling (Tamura et al., 2000), raising the possibility that this peptide could be involved in aspects of maternal vascular responses to pregnancy that are impaired in sPE.

In summary, we studied the impact of sPE on the CTB layer of the smooth chorion. In comparison to the equivalent region in nPTB, we found a large number of differences at morphological and functional levels. We also found that sPE had very different effects on the chorion frondosum and the chorion laeve, possible evidence that the CTBs in the two areas are different subpopulations of cells. The results also raised the possibility of crosstalk between the two extra-embryonic regions that enabled the smooth chorion to compensate for deficits in the villous placenta. In this new light, we propose that CTBs that reside in the fetal membranes play a larger role in governing pregnancy outcome than was previously appreciated.

MATERIALS AND METHODS

Human tissue collection

The UCSF Institutional Review Board approved this study. Informed consent was obtained from all donors. Samples were collected within 1 h of the procedure, washed in PBS and kept in cytowash medium (DME/H-21 medium, 1% Glutamine Plus, 1% penicillin/streptomycin, 0.1% gentamycin) supplemented with 2.5% fetal bovine serum (FBS), placed on ice prior to processing. The second trimester samples were classified as early (15.5 to 17.6 weeks), mid (18 to 22.3 weeks) or late (22.4 to 24 weeks). The clinical characteristics of the sPE and nPTB pregnancies are summarized in Tables S1 and S2.

Immunolocalization

Immunolocalization was carried out using previously published methods (Genbacev et al., 2016). The antibodies we employed are listed in Table S3 along with the working concentrations.

Morphological evaluations of the smooth chorion

All biopsies (~10×20-40 mm) were obtained either 5-10 cm (second trimester) or 10-15 cm (term) from the chorionic plate, from random areas of the smooth chorion (at least three per case). They were washed in PBS, fixed with 4% paraformaldehyde for 30 min and infiltrated with 5-15% sucrose. The samples were rolled end-to-end, embedded in OCT, and frozen in liquid nitrogen. Tissue sections from second trimester, sPE and nPTB samples (n=5/each group) were stained with H&E.

Immunolocalization of cytokeratin and vimentin was performed as described (Genbacev et al., 2016). Tilescan images of the entire tissue section were generated using a Leica DMI6000 B fluorescence microscope (Leica Microsystems) and LAS software. This method enabled evaluation of a large area of the tissue (~10-30×1 mm wide). All measurements were performed using ImageJ (version 1.45s). Three sections from two areas of early second trimester (n=3), mid second trimester (n=4), late second trimester (n=3), sPE (n=5) or nPTB (n=5) specimens were examined. The width of the CTB layer was measured from the inner edge of CTBs adjacent to the stroma to the outer edge, which was adjacent to the decidua. Ten random measurements were made over the entire length of the samples. In parallel, GV in the same images were counted using ImageJ.

Development (2017) 144, 767-777 doi:10.1242/dev.146100

Isolation of villous cytotrophoblasts

vCTBs were isolated from second and third trimester human placentas by published methods (Fisher et al., 1989; Kliman and Feinberg, 1990). Primary CTBs were from floating (second trimester and term) and anchoring (second trimester) villi, which were dissected from the placentas. The isolated cytotrophoblasts were ≥90% pure as shown by staining for cytokeratin 7.

Isolation of schCTBs

After extensive washing with 1× PBS (Ca^{2+} and Mg^{2+} free) supplemented with 1% penicillin-streptomycin (100× stock solution; 10,000 units/ml penicillin and 10,000 µg/ml streptomycin), 0.003% fungizone (stock solution of 250 mg/ml) and 1% gentamicin, the amnion and smooth chorion were manually separated along their shared stromal plane. Next, the decidua parietalis was removed and discarded. The chorionic CTB layer was minced into small pieces (3-4 mm) and subjected to a series of enzyme digestion steps. The first incubation (15-30 min) was in PBS (10 ml/g of tissue) containing 3.5 mg collagenase, 1.2 mg DNase, 6.9 mg hyaluronidase and 10 mg bovine serum albumin. The supernatant was discarded. Then, the tissue was incubated for 20-40 min in PBS containing trypsin (6.9 mg trypsin, 20 mg EDTA, 12 mg DNase per 100 ml; tissue weight: dissociation buffer volume=1:8). Enzyme activity was stopped by adding an equal volume of cytowash containing 10% FBS. The cell suspension was filtered through a 70 µm sterile strainer and centrifuged at 1200 ***g*** for 7 min. A second collagenase digestion was performed by adding a 7× volume of the collagenase digestion buffer (see above), calculated on the basis of the weight of the cell pellet, followed by incubation for 15-30 min. The cell suspension was collected a second time by centrifugation. The cell pellets from the trypsin and second collagenase digestions were combined and purified over a Percoll gradient as described above for vCTBs.

Invasion assays

CTB invasion was quantified by using our previously published methods (Genbacev et al., 2016). The entire experiment was repeated three to four times per group. Two inserts were evaluated for each sample type.

Laser microdissection

We used laser capture microdissection to isolate schCTBs from normal second trimester, sPE or nPTB smooth chorion samples (n=4/each group). Portions of the smooth chorion, separated from the amnion as described above, were washed repeatedly in cold PBS to remove blood. Unfixed specimens were rolled end-to-end, placed in cryomolds containing OCT, frozen over a dry ice/ethanol slurry, and stored at −80°C. The blocks were sectioned at 20 µm using a Leica CM3050 cryostat, mounted on UV-treated PEN-membrane slides (ThermoFisher Scientific), and stored under ice prior to laser capture microdissection later that day.

Immediately prior to the procedure, sections were immersed in cold PBS until the OCT dissolved (~1 min), dipped in 0.1% Toluidine Blue for 30 s, washed in cold PBS, dehydrated (30 s/treatment) in a graded ethanol series (75%, 95%, 100%), then rapidly dried with compressed nitrogen. All solutions were made with nuclease-free water.

schCTBs were laser dissected (Leica LMD 7000) and collected directly into RLT Plus Buffer (Qiagen RNeasy Plus Micro kit).

Total RNA was isolated according to the manufacturer's protocol and concentrations were measured photometrically (NanoDrop 2000c). RNA integrity was determined via microfluidic phoresis (Agilent Bioanalyzer 2100). The samples were stored at −80°C.

Microarray analyses

Global gene profiling was accomplished using the GeneChip HuGene 2.0 ST array (Affymetrix). Sample processing and hybridization were carried out according to protocols that were devised by the UCSF Gladstone (NHLBI) Genomics Core Facility. Gene level expression data quality was confirmed, normalized (RMA) and summarized (Affymetrix Expression Console Software). Significant differential expression was determined by statistical analysis of false discovery rate (FDR<0.05) and absolute linear fold change >2 (Transcriptome Analysis Console Software).

PAPPA1 ELISA

Sch- and vCTB-conditioned medium was isolated from sPE (n=3) and control nPTB (n=3) samples. The PAPPA1 concentrations of technical replicates were assayed by using a commercial ELISA kit (LifeSpan BioSciences) according to the manufacturer's instructions. Sample values (pg/ml) were extrapolated from the standard curve.

IGF1-induced CTB proliferation

Freshly isolated second trimester vCTBs and schCTBs were plated at a density of 8400 cells per well of a 96-well plate coated with Matrigel diluted 1:2 in medium containing various concentrations of human recombinant IGF1 (291-G1-200, R&D Systems): 0, 2, 10, 50 and 75 ng/ml. BrDU (60 µM) was added simultaneously. After 16 h, BrDU incorporation was assessed according to the manufacturer's directions (ab126556, Abcam, UK). The entire experiment was repeated three times with duplicate or triplicate technical replicates.

Statistical analysis

Data are shown as mean±s.e.m. Student's one-tailed t-distribution was used to compare the mean values among groups. Statistical significance was defined as P<0.05.

Acknowledgements

We are grateful to Dr Mari-Paule Thiet and the UCSF Maternal-Fetal Medicine Division for invaluable help in obtaining placental and fetal membrane samples that made this study possible. We also thank the recruiters for this study: Lisa Wilson, Lisa Gertridge, Allison O'Leary, Stephanie Leong, Jean Perry and Rachel Freyre. We are indebted to the patient participants. We are grateful to Dr Michael McMaster for critical reading of the manuscript and help with preparation of the figures.

Competing interests

The authors declare no competing or financial interests.

Author contributions

T.G.-G., K.O. and M.K. performed the experiments. M.G. prepared the samples for global transcriptional profiling and analyzed the data. C.S., O.G. and S.J.F. designed the experiments. O.G. and S.J.F. guided their execution. All authors contributed to the interpretation of the data. T.G.-G., K.O. and M.G. prepared the figures and tables. T.G.-G. and S.J.F. wrote the manuscript, which the other authors helped edit.

Funding

T.G.-G. was the recipient of a fellowship from the Instituto de Salud Carlos III, through the Sara Borrell Programme (CD14/00229). Research reported in this publication was supported by the Eunice Kennedy Shriver National Institute of Child Health & Human Development of the National Institutes of Health under awards P50HD055764 and R37HD076253. Deposited in PMC for immediate release.

Data availability

Microarray data have been deposited in Gene Expression Omnibus under accession number GSE91189 (https://www.ncbi.nlm.nih.gov/geo/query/acc.cgi?acc=GSE91189).

Supplementary information

Supplementary information available online at http://dev.biologists.org/lookup/doi/10.1242/dev.146100.supplemental

References

Abitbol, M. M., Ober, M. B., Gallo, G. R., Driscoll, S. G. and Pirani, C. L. (1977). Experimental toxemia of pregnancy in the monkey, with a preliminary report on renin and aldosterone. *Am. J. Pathol.* **86**, 573-590.

Amaral, L. M., Cornelius, D. C., Harmon, A., Moseley, J., Martin, J. N., Jr and LaMarca, B. (2015). 17-hydroxyprogesterone caproate significantly improves clinical characteristics of preeclampsia in the reduced uterine perfusion pressure rat model. *Hypertension* **65**, 225-231.

Behzad, F., Jones, C. J. P., Ball, S., Alvares, T. and Aplin, J. D. (1995). Studies of hemidesmosomes in human amnion: the use of a detergent extraction protocol for compositional and ultrastructural analysis and preparation of a hemidesmosome-enriched fraction from tissue. *Acta Anat.* **152**, 170-184.

Benirschke, K., Burton, G. and Baergen, R. N. (2012). *Pathology of the Human Placenta*. p. 1. online resource. Berlin: Springer.
Brosens, I. A., Robertson, W. B. and Dixon, H. G. (1970). The role of the spiral arteries in the pathogenesis of pre-eclampsia. *J. Pathol.* **101**, Pvi.
Bulmer, J. N., Thrower, S. and Wells, M. (1989). Expression of epidermal growth factor receptor and transferrin receptor by human trophoblast populations. *Am. J. Reprod. Immunol.* **21**, 87-93.
Burton, G. J. and Jauniaux, E. (2015). What is the placenta? *Am. J. Obstet. Gynecol.* **213**, S6.e1-S6.e4.
Burton, G. J., Jauniaux, E. and Charnock-Jones, D. S. (2010). The influence of the intrauterine environment on human placental development. *Int. J. Dev. Biol.* **54**, 303-312.
Damsky, C. H., Librach, C., Lim, K. H., Fitzgerald, M. L., McMaster, M. T., Janatpour, M., Zhou, Y., Logan, S. K. and Fisher, S. J. (1994). Integrin switching regulates normal trophoblast invasion. *Development* **120**, 3657-3666.
Enders, A. C., Blankenship, T. N., Fazleabas, A. T. and Jones, C. J. P. (2001). Structure of anchoring villi and the trophoblastic shell in the human, baboon and macaque placenta. *Placenta* **22**, 284-303.
Fisher, S. J., Cui, T. Y., Zhang, L., Hartman, L., Grahl, K., Zhang, G. Y., Tarpey, J. and Damsky, C. H. (1989). Adhesive and degradative properties of human placental cytotrophoblast cells in vitro. *J. Cell Biol.* **109**, 891-902.
Floridon, C., Nielsen, O., Holund, B., Sweep, F., Sunde, L., Thomsen, S. G. and Teisner, B. (2000). Does plasminogen activator inhibitor-1 (PAI-1) control trophoblast invasion? A study of fetal and maternal tissue in intrauterine, tubal and molar pregnancies. *Placenta* **21**, 754-762.
Gaidamauskas, E., Gyrup, C., Boldt, H. B., Schack, V. R., Overgaard, M. T., Laursen, L. S. and Oxvig, C. (2013). IGF dependent modulation of IGF binding protein (IGFBP) proteolysis by pregnancy-associated plasma protein-A (PAPP-A): multiple PAPP-A-IGFBP interaction sites. *Biochim. Biophys. Acta* **1830**, 2701-2709.
Genbacev, O., Vićovac, L. and Larocque, N. (2015). The role of chorionic cytotrophoblasts in the smooth chorion fusion with parietal decidua. *Placenta* **36**, 716-722.
Genbacev, O., Larocque, N., Ona, K., Prakobphol, A., Garrido-Gomez, T., Kapidzic, M., Bárcena, A., Gormley, M. and Fisher, S. J. (2016). Integrin alpha4-positive human trophoblast progenitors: functional characterization and transcriptional regulation. *Hum. Reprod.* **31**, 1300-1314.
Granger, J. P., LaMarca, B. B., Cockrell, K., Sedeek, M., Balzi, C., Chandler, D. and Bennett, W. (2006). Reduced uterine perfusion pressure (RUPP) model for studying cardiovascular-renal dysfunction in response to placental ischemia. *Methods Mol. Med.* **122**, 383-392.
Handwerger, S. and Freemark, M. (2000). The roles of placental growth hormone and placental lactogen in the regulation of human fetal growth and development. *J. Pediatr. Endocrinol. Metab.* **13**, 343-356.
Hu, Y., Wang, J., Yang, B., Zheng, N., Qin, M., Ji, Y., Lin, G., Tian, L., Wu, X., Wu, L. et al. (2011). Guanylate binding protein 4 negatively regulates virus-induced type I IFN and antiviral response by targeting IFN regulatory factor 7. *J. Immunol.* **187**, 6456-6462.
Hustin, J., Foidart, J. M. and Lambotte, R. (1984). Cellular proliferation in villi of normal and pathological pregnancies. *Gynecol. Obstet. Invest.* **17**, 1-9.
Ishida-Yamamoto, A. and Igawa, S. (2015). The biology and regulation of corneodesmosomes. *Cell Tissue Res.* **360**, 477-482.
Johansson, A.-S. and Mannervik, B. (2001). Human glutathione transferase A3-3, a highly efficient catalyst of double-bond isomerization in the biosynthetic pathway of steroid hormones. *J. Biol. Chem.* **276**, 33061-33065.
Kliman, H. J. and Feinberg, R. F. (1990). Human trophoblast-extracellular matrix (ECM) interactions in vitro: ECM thickness modulates morphology and proteolytic activity. *Proc. Natl. Acad. Sci. USA* **87**, 3057-3061.
Kramer, A. W., Lamale-Smith, L. M. and Winn, V. D. (2016). Differential expression of human placental PAPP-A2 over gestation and in preeclampsia. *Placenta* **37**, 19-25.
Krapp, C., Hotter, D., Gawanbacht, A., McLaren, P. J., Kluge, S. F., Stürzel, C. M., Mack, K., Reith, E., Engelhart, S., Ciuffi, A. et al. (2016). Guanylate Binding Protein (GBP) 5 is an interferon-inducible inhibitor of HIV-1 infectivity. *Cell Host Microbe* **19**, 504-514.
Lalani, E.-N. M. A., Bulmer, J. N. and Wells, M. (1987). Peroxidase-labelled lectin binding of human extravillous trophoblast. *Placenta* **8**, 15-26.
Lenz, T., Sealey, J. E. and Tewksbury, D. A. (1993). Regional distribution of the angiotensinogens in human placentae. *Placenta* **14**, 695-699.
Lim, K. H., Zhou, Y., Janatpour, M., McMaster, M., Bass, K., Chun, S. H. and Fisher, S. J. (1997). Human cytotrophoblast differentiation/invasion is abnormal in pre-eclampsia. *Am. J. Pathol.* **151**, 1809-1818.
Maltepe, E. and Fisher, S. J. (2015). Placenta: the forgotten organ. *Annu. Rev. Cell Dev. Biol.* **31**, 523-552.
Männik, J., Vaas, P., Rull, K., Teesalu, P. and Laan, M. (2012). Differential placental expression profile of human Growth Hormone/Chorionic Somatomammotropin genes in pregnancies with pre-eclampsia and gestational diabetes mellitus. *Mol. Cell. Endocrinol.* **355**, 180-187.
Poisner, A. M., Wood, G. W., Poisner, R. and Inagami, T. (1981). Localization of renin in trophoblasts in human chorion laeve at term pregnancy. *Endocrinology* **109**, 1150-1155.
Redman, C. W. and Sargent, I. L. (2005). Latest advances in understanding preeclampsia. *Science* **308**, 1592-1594.
Shenoy, A. R., Wellington, D. A., Kumar, P., Kassa, H., Booth, C. J., Cresswell, P. and MacMicking, J. D. (2012). GBP5 promotes NLRP3 inflammasome assembly and immunity in mammals. *Science* **336**, 481-485.
Symonds, E. M., Stanley, M. A. and Skinner, S. L. (1968). Production of renin by in vitro cultures of human chorion and uterine muscle. *Nature* **217**, 1152-1153.
Tamura, N., Ogawa, Y., Chusho, H., Nakamura, K., Nakao, K., Suda, M., Kasahara, M., Hashimoto, R., Katsuura, G., Mukoyama, M. et al. (2000). Cardiac fibrosis in mice lacking brain natriuretic peptide. *Proc. Natl. Acad. Sci. USA* **97**, 4239-4244.
Tyrkalska, S. D., Candel, S., Angosto, D., Gómez-Abellán, V., Martín-Sánchez, F., García-Moreno, D., Zapata-Pérez, R., Sánchez-Ferrer, A., Sepulcre, M. P., Pelegrín, P. et al. (2016). Neutrophils mediate Salmonella Typhimurium clearance through the GBP4 inflammasome-dependent production of prostaglandins. *Nat. Commun.* **7**, 12077.
Yeh, I.-T., O'Connor, D. M. and Kurman, R. J. (1989). Vacuolated cytotrophoblast: a subpopulation of trophoblast in the chorion laeve. *Placenta* **10**, 429-438.
You, H. J., Lee, K. J. and Jeong, H. G. (2002). Overexpression of human metallothionein-III prevents hydrogen peroxide-induced oxidative stress in human fibroblasts. *FEBS Lett.* **521**, 175-179.
Yuan, B., Ohyama, K., Bessho, T. and Toyoda, H. (2006). Contribution of inducible nitric oxide synthase and cyclooxygenase-2 to apoptosis induction in smooth chorion trophoblast cells of human fetal membrane tissues. *Biochem. Biophys. Res. Commun.* **341**, 822-827.
Yuan, B., Ohyama, K., Bessho, T., Uchide, N. and Toyoda, H. (2008). Imbalance between ROS production and elimination results in apoptosis induction in primary smooth chorion trophoblast cells prepared from human fetal membrane tissues. *Life Sci.* **82**, 623-630.
Yuan, B., Ohyama, K., Takeichi, M. and Toyoda, H. (2009). Direct contribution of inducible nitric oxide synthase expression to apoptosis induction in primary smooth chorion trophoblast cells of human fetal membrane tissues. *Int. J. Biochem. Cell Biol.* **41**, 1062-1069.
Zhou, Y., Damsky, C. H., Chiu, K., Roberts, J. M. and Fisher, S. J. (1993). Preeclampsia is associated with abnormal expression of adhesion molecules by invasive cytotrophoblasts. *J. Clin. Invest.* **91**, 950-960.
Zhou, Y., Damsky, C. H. and Fisher, S. J. (1997). Preeclampsia is associated with failure of human cytotrophoblasts to mimic a vascular adhesion phenotype. One cause of defective endovascular invasion in this syndrome? *J. Clin. Invest.* **99**, 2152-2164.
Zhou, Y., Gormley, M. J., Hunkapiller, N. M., Kapidzic, M., Stolyarov, Y., Feng, V., Nishida, M., Drake, P. M., Bianco, K., Wang, F. et al. (2013). Reversal of gene dysregulation in cultured cytotrophoblasts reveals possible causes of preeclampsia. *J. Clin. Invest.* **123**, 2862-2872.

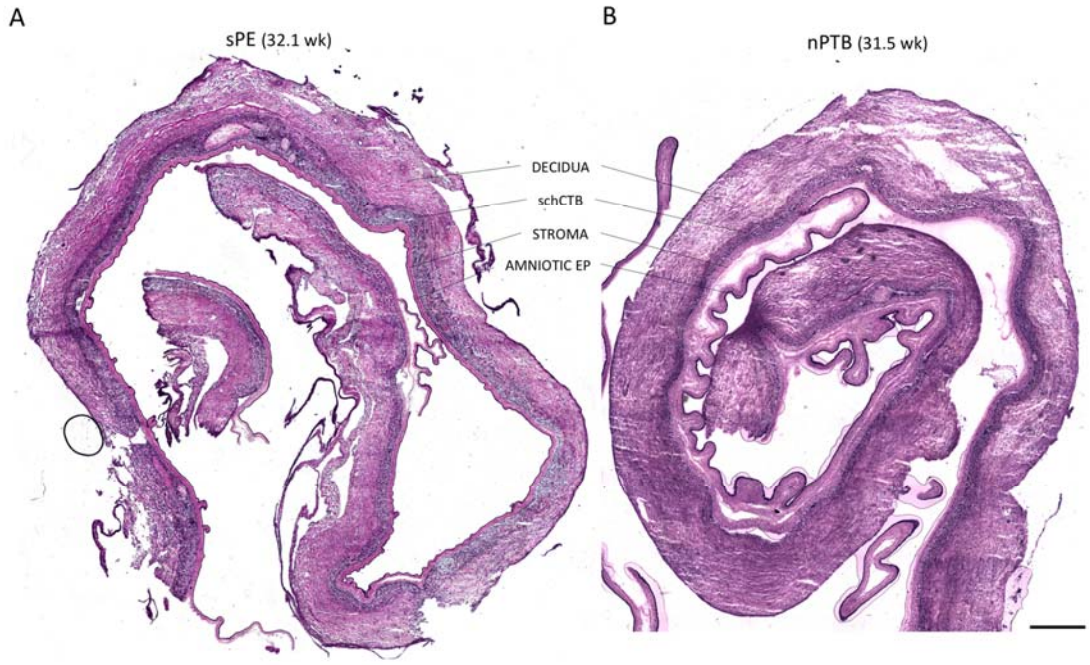

Supplemental Figure 1. Low power micrograph of H&E stained fetal membranes showed that severe preeclampsia (sPE) was associated with expansion of the CTB layer of the smooth chorion (schCTB), a phenomenon which was not observed in equivalent samples form cases of non infected preterm birth. n=5/group; scale bar: 500 μm.

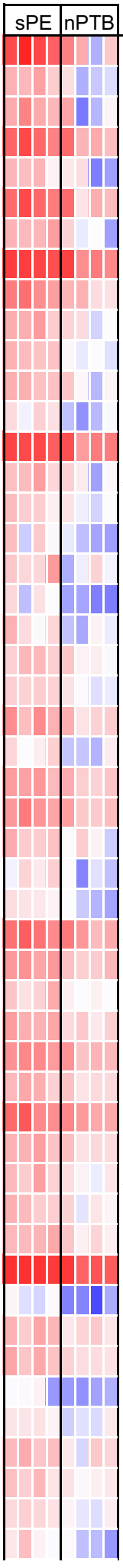

Symbol	Title	Δ
CSH1	chorionic somatomammotropin hormone 1	26
GSTA3	glutathione S-transferase alpha 3	13
T1560	T1560 protein	12
PAPPA	pregnancy-associated plasma protein A, pappalysin 1	9
XX-C2158C6.3	putative novel transcript	8
HTRA4	HtrA serine peptidase 4	8
PDIA3P1	protein disulfide isomerase family A, member 3 pseudogene 1	8
PAPPA-AS1	PAPPA antisense RNA 1	7
CSH2	chorionic somatomammotropin hormone 2	7
RP11-78C3.1	novel transcript	6
RNU2-63P	RNA, U2 small nuclear 63, pseudogene	6
TGFBR3L	transforming growth factor, beta receptor III-like	6
RP11-327J17.2	novel transcript	5
PAPPA2	pappalysin 2	4
AC004878.2	novel transcript	4
LOC389765	kinesin family member 27 pseudogene	4
LINC01028	long intergenic non-protein coding RNA 1028	4
SCARNA9L	small Cajal body-specific RNA 9-like	4
FAR2P3	fatty acyl CoA reductase 2 pseudogene 3	4
SNORD114-28	small nucleolar RNA, C/D box 114-28	4
GDPD1	glycerophosphodiester phosphodiesterase domain containing 1	4
CHRM5	cholinergic receptor, muscarinic 5	4
KCNJ16	potassium inwardly-rectifying channel, subfamily J, member 16	4
RP11-246A10.1	novel transcript	4
RECK	reversion-inducing-cysteine-rich protein with kazal motifs	4
PDIA5	protein disulfide isomerase family A, member 5	4
PSG11	pregnancy specific beta-1-glycoprotein 11	4
RAB9BP1	RAB9B, member RAS oncogene family pseudogene 1	4
LINC01338	long intergenic non-protein coding RNA 1338	4
ADAM12	ADAM metallopeptidase domain 12	4
FBXO9	F-box protein 9	4
DGCR11	DiGeorge syndrome critical region gene 11 (non-protein coding)	3
SNORD8	small nucleolar RNA, C/D box 8	3
MAP7D3	MAP7 domain containing 3	3
SLC23A2	solute carrier family 23 (ascorbic acid transporter), member 2	3
LIFR	leukemia inhibitory factor receptor alpha	3
HYAL4	hyaluronoglucosaminidase 4	3
AC004878.8	novel transcript	3
GPR126	G protein-coupled receptor 126	3
FGG	fibrinogen gamma chain	3
HEXB	hexosaminidase B (beta polypeptide)	3
RNU6-989P	RNA, U6 small nuclear 989, pseudogene	3
POTEE	POTE ankyrin domain family, member E	3
POTEF	POTE ankyrin domain family, member F	3
MIR924	microRNA 924	3
RP4-693M11.3	novel transcript, antisense to DNAL1	3
NAIP	NLR family, apoptosis inhibitory protein	3
DDX43	DEAD (Asp-Glu-Ala-Asp) box polypeptide 43	3
SNORA6	small nucleolar RNA, H/ACA box 6	3
MEP1A	meprin A, alpha (PABA peptide hydrolase)	3

sPE	nPTB	Symbol	Title	Δ
		PDPR	pyruvate dehydrogenase phosphatase regulatory subunit	3
		BGN	biglycan	3
		LOC440173	uncharacterized LOC440173	3
		LOC101926943	uncharacterized LOC101926943	3
		RNU12	RNA, U12 small nuclear	3
		RNA5SP435	RNA, 5S ribosomal pseudogene 435	3
		SH3BP5-AS1	SH3BP5 antisense RNA 1	3
		CTD-2363C16.1	novel transcript	3
		C8orf48	chromosome 8 open reading frame 48	3
		LRRC17	leucine rich repeat containing 17	3
		RNU7-123P	RNA, U7 small nuclear 123 pseudogene	3
		ZNF283	zinc finger protein 283	3
		KCNJ2	potassium inwardly-rectifying channel, subfamily J, member 2	3
		ITM2C	integral membrane protein 2C	3
		SUN3	Sad1 and UNC84 domain containing 3	2
		LOC220729	succinate dehydrogenase complex, subunit A, flavoprotein (Fp) pseudogene	2
		KRT223P	keratin 223 pseudogene	2
		CXorf58	chromosome X open reading frame 58	2
		LOC100506922	basic proline-rich protein-like	2
		EXO5	exonuclease 5	2
		SMAD4	SMAD family member 4	2
		ENG	endoglin	2
		RP11-288L9.1	putative novel transcript	2
		TSPAN10	tetraspanin 10	2
		LOC100506746	uncharacterized LOC100506746	2
		MIR3942	microRNA 3942	2
		MT1F	metallothionein 1F	2
		MKLN1-AS	MKLN1 antisense RNA	2
		MAGEH1	melanoma antigen family H, 1	2
		LOC101928062	uncharacterized LOC101928062	2
		PCBD2	pterin-4 alpha-carbinolamine dehydratase/dimerization cofactor of hepatocyte nuclear factor 1 alpha (TCF1) 2	2
		TDRD6	tudor domain containing 6	2
		ZNF594	zinc finger protein 594	2
		ICA1L	islet cell autoantigen 1,69kDa-like	2
		SPATA17	spermatogenesis associated 17	2
		NBPF1	neuroblastoma breakpoint family, member 1	2
		PTPRQ	protein tyrosine phosphatase, receptor type, Q	2
		RNU6-806P	RNA, U6 small nuclear 806, pseudogene	2
		RPS6KA6	ribosomal protein S6 kinase, 90kDa, polypeptide 6	2
		RP11-317G6.1	novel transcript, antisense to HERC1	2
		SLC29A3	solute carrier family 29 (equilibrative nucleoside transporter), member 3	2
		CABLES1	Cdk5 and Abl enzyme substrate 1	2
		ATP8A2	ATPase, aminophospholipid transporter, class I, type 8A, member 2	2
		MIR4759	microRNA 4759	2
		HDAC5	histone deacetylase 5	2
		TGIF2LY	TGFB-induced factor homeobox 2-like, Y-linked	2
		EOGT	EGF domain-specific O-linked N-acetylglucosamine (GlcNAc) transferase	2
		SCG2	secretogranin II	2
		ERVV-2	endogenous retrovirus group V, member 2	2
		TCEA3	transcription elongation factor A (SII), 3	2

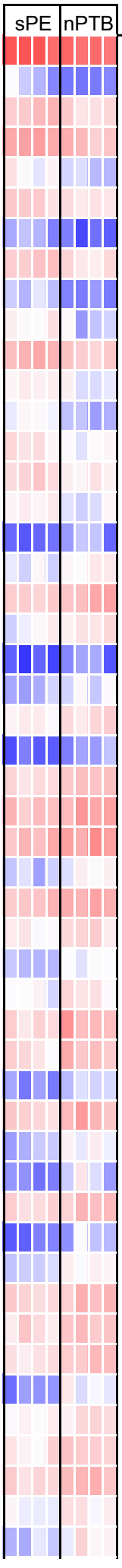

Symbol	Title	Δ
TNKS2	tankyrase, TRF1-interacting ankyrin-related ADP-ribose polymerase 2	2
RNU6-858P	RNA, U6 small nuclear 858, pseudogene	2
RP11-545P7.4	novel transcript, antisense to C12orf52	2
LINC01003	long intergenic non-protein coding RNA 1003	2
CROCCP3	ciliary rootlet coiled-coil, rootletin pseudogene 3	2
ZFYVE9	zinc finger, FYVE domain containing 9	2
RNU6-77P	RNA, U6 small nuclear 77, pseudogene	2
HABP4	hyaluronan binding protein 4	2
OR10A3	olfactory receptor, family 10, subfamily A, member 3	2
RP1-50J22.4	putative novel transcript	2
SH3BP5	SH3-domain binding protein 5 (BTK-associated)	2
SPATA17-AS1	SPATA17 antisense RNA 1	2
USP50	ubiquitin specific peptidase 50	2
DCLRE1C	DNA cross-link repair 1C	2
PROSC	proline synthetase co-transcribed homolog (bacterial)	2
RP11-585P4.5	novel transcript, antisense to GLIPR1	2
CTD-2501M5.1	novel transcript	-2
KIAA1958	KIAA1958	-2
NNMT	nicotinamide N-methyltransferase	-2
RNA5SP356	RNA, 5S ribosomal pseudogene 356	-2
RNU6-557P	RNA, U6 small nuclear 557, pseudogene	-2
LOC100129617	uncharacterized LOC100129617	-2
P2RY6	pyrimidinergic receptor P2Y, G-protein coupled, 6	-2
RNU6-1157P	RNA, U6 small nuclear 1157, pseudogene	-2
TRIM22	tripartite motif containing 22	-2
MAST4	microtubule associated serine/threonine kinase family member 4	-2
HLA-B	major histocompatibility complex, class I, B	-2
CD80	CD80 molecule	-2
HLA-A	major histocompatibility complex, class I, A	-2
IL10RA	interleukin 10 receptor, alpha	-2
EPHA5-AS1	EPHA5 antisense RNA 1	-2
RP11-217B7.2	novel transcript	-2
NPPB	natriuretic peptide B	-2
HMMR	hyaluronan-mediated motility receptor (RHAMM)	-2
LOC102723672	uncharacterized LOC102723672	-2
PSTPIP2	proline-serine-threonine phosphatase interacting protein 2	-2
ITK	IL2-inducible T-cell kinase	-2
RNA5SP234	RNA, 5S ribosomal pseudogene 234	-2
CASP4	caspase 4, apoptosis-related cysteine peptidase	-2
MIR1204	microRNA 1204	-2
LINC01057	long intergenic non-protein coding RNA 1057	-2
CNN3	calponin 3, acidic	-2
SNAR-C2	small ILF3/NF90-associated RNA C2	-2
TMEM52B	transmembrane protein 52B	-2
RNA5SP88	RNA, 5S ribosomal pseudogene 88	-2
RASA3	RAS p21 protein activator 3	-2
KRT17P1	keratin 17 pseudogene 1	-2
NUAK2	NUAK family, SNF1-like kinase, 2	-2
RNA5-8SP3	RNA, 5.8S ribosomal pseudogene 3	-2
SNORA84	small nucleolar RNA, H/ACA box 84	-2

sPE	nPTB	Symbol	Title	Δ
		CLDN6	claudin 6	-2
		RNA5SP22	RNA, 5S ribosomal pseudogene 22	-2
		EPCAM	epithelial cell adhesion molecule	-2
		IFITM1	interferon induced transmembrane protein 1	-2
		RNU6-707P	RNA, U6 small nuclear 707, pseudogene	-2
		CD47	CD47 molecule	-2
		LOC391003	PRAME family member-like	-2
		TAP1	transporter 1, ATP-binding cassette, sub-family B (MDR/TAP)	-2
		SLC44A3	solute carrier family 44, member 3	-2
		YBX3P1	Y box binding protein 3 pseudogene 1	-2
		HIST1H2AE	histone cluster 1, H2ae	-2
		RNU6-74P	RNA, U6 small nuclear 74, pseudogene	-2
		IL4R	interleukin 4 receptor	-2
		RP11-290L1.3	novel transcript antisense to PHLDA1	-2
		SLAMF8	SLAM family member 8	-2
		IL2RG	interleukin 2 receptor, gamma	-3
		PLAUR	plasminogen activator, urokinase receptor	-3
		RP11-10J5.1	putative novel transcript	-3
		VTRNA1-3	vault RNA 1-3	-3
		RP11-212I21.2	novel transcript	-3
		SNORD50B	small nucleolar RNA, C/D box 50B	-3
		IRF1	interferon regulatory factor 1	-3
		CD96	CD96 molecule	-3
		MIR3529	microRNA 3529	-3
		C6orf48	chromosome 6 open reading frame 48	-3
		DRAM1	DNA-damage regulated autophagy modulator 1	-3
		HIST1H3F	histone cluster 1, H3f	-3
		PLAU	plasminogen activator, urokinase	-3
		NEAT1	nuclear paraspeckle assembly transcript 1 (non-protein coding) (microRNA 612)	-3
		RP4-694A7.2	putative novel transcript	-3
		SNORD52	small nucleolar RNA, C/D box 52	-3
		CCL4	chemokine (C-C motif) ligand 4	-3
		CD48	CD48 molecule	-3
		XXbac-BPG252P9	novel transcript antisense to IER3	-3
		RNY4P20	RNA, Ro-associated Y4 pseudogene 20	-3
		RNU6-1316P	RNA, U6 small nuclear 1316, pseudogene	-3
		ANKRD54	ankyrin repeat domain 54	-3
		SKA3	spindle and kinetochore associated complex subunit 3	-3
		GZMB	granzyme B (granzyme 2, cytotoxic T-lymphocyte-associated serine esterase 1)	-3
		RNU4-62P	RNA, U4 small nuclear 62, pseudogene	-3
		RNU6-1187P	RNA, U6 small nuclear 1187, pseudogene	-3
		RP1-239B22.5	antisense to KCNJ11 and overlapping to a novel gene	-3
		GBP1P1	guanylate binding protein 1, interferon-inducible pseudogene 1	-3
		SQRDL	sulfide quinone reductase-like (yeast)	-3
		RNU6-226P	RNA, U6 small nuclear 226, pseudogene	-3
		CXCL2	chemokine (C-X-C motif) ligand 2	-3
		HIST1H2AK	histone cluster 1, H2ak	-3
		MIR28	microRNA 28	-3
		MIR3671	microRNA 3671	-3
		RP11-102L12.2	novel transcript antisense to RASGRP1	-3

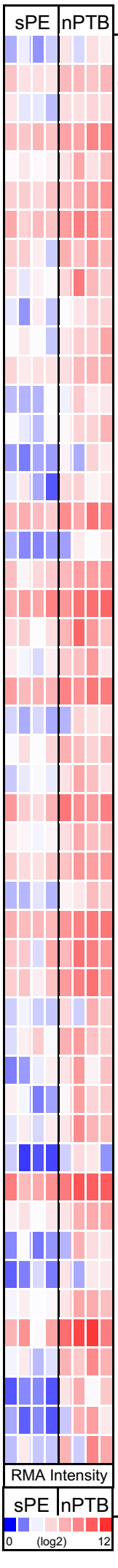

Symbol	Title	Δ
RNU6-1330P	RNA, U6 small nuclear 1330, pseudogene	-3
AREG	amphiregulin	-3
HIST1H4L	histone cluster 1, H4l	-3
GBP2	guanylate binding protein 2, interferon-inducible	-3
C10orf55	chromosome 10 open reading frame 55	-3
SOCS3	suppressor of cytokine signaling 3	-3
HIST1H3I	histone cluster 1, H3i	-3
MIR1323	microRNA 1323	-3
LOC541472	uncharacterized LOC541472	-4
SNORD16	small nucleolar RNA, C/D box 16	-4
SOCS1	suppressor of cytokine signaling 1	-4
SIPA1L1	signal-induced proliferation-associated 1 like 1	-4
RP11-92K15.1	novel transcript	-4
FOSL1	FOS-like antigen 1	-4
MIR302A	microRNA 302a	-4
RNU6-890P	RNA, U6 small nuclear 890, pseudogene	-4
GBP1	guanylate binding protein 1, interferon-inducible	-4
SNORA29	small nucleolar RNA, H/ACA box 29	-4
SNORD63	small nucleolar RNA, C/D box 63	-4
JUNB	jun B proto-oncogene	-4
CCL4L2	chemokine (C-C motif) ligand 4-like 2	-4
SLAMF7	SLAM family member 7	-4
KRT17	keratin 17	-4
RNU6-638P	RNA, U6 small nuclear 638, pseudogene	-4
CCL13	chemokine (C-C motif) ligand 13	-4
KLHL22-IT1	KLHL22 intronic transcript 1 (non-protein coding)	-5
CD24	CD24 molecule	-5
BCL2A1	BCL2-related protein A1	-5
FGFR2	fibroblast growth factor receptor 2	-5
HRASLS2	HRAS-like suppressor 2	-5
ITGA2	integrin, alpha 2 (CD49B, alpha 2 subunit of VLA-2 receptor)	-5
CCL2	chemokine (C-C motif) ligand 2	-5
CCL5	chemokine (C-C motif) ligand 5	-6
CD3D	CD3d molecule, delta (CD3-TCR complex)	-6
LINC00278	long intergenic non-protein coding RNA 278	-6
SNORD75	small nucleolar RNA, C/D box 75	-6
MIR548K	microRNA 548k	-6
ICAM1	intercellular adhesion molecule 1	-6
RNU6-767P	RNA, U6 small nuclear 767, pseudogene	-6
OLR1	oxidized low density lipoprotein (lectin-like) receptor 1	-7
BMP2	bone morphogenetic protein 2	-7
RP1-67K17.4	putative novel transcript	-7
RNU6-874P	RNA, U6 small nuclear 874, pseudogene	-7
PMAIP1	phorbol-12-myristate-13-acetate-induced protein 1	-8
CXCL10	chemokine (C-X-C motif) ligand 10	-9
GBP4	guanylate binding protein 4	-9
SNORD59A	small nucleolar RNA, C/D box 59A	-12
RNU6-1154P	RNA, U6 small nuclear 1154, pseudogene	-14
GBP5	guanylate binding protein 5	-20

Symbol	Title	Δ

Supplemental Figure 2. Global transcriptional profiling of cytotrophoblasts from the smooth chorion revealed sPE-associated aberrations in gene expression as compared to the equivalent subpopulation of cells from cases of non-infected preterm birth. The heatmap lists genes that were differentially expressed by 2-fold or greater. The fold changes are shown on the right (.)Δ

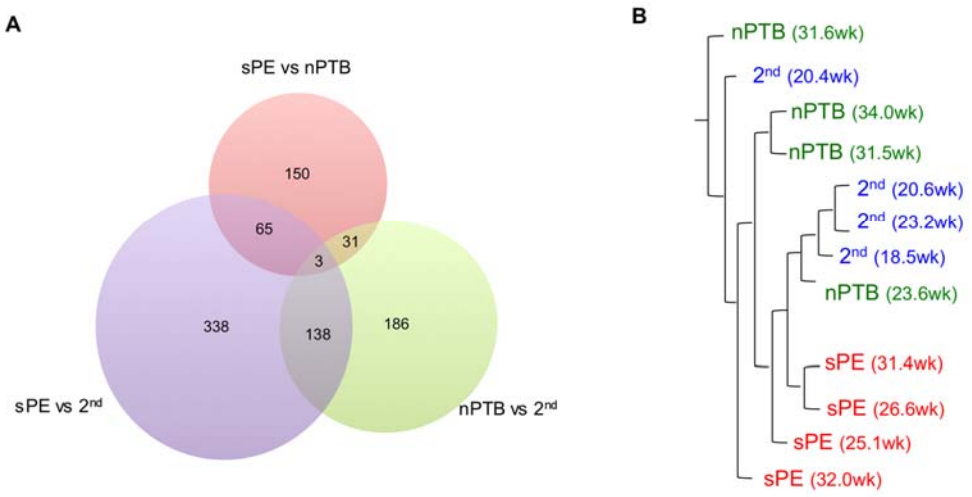

Supplemental Figure 3. Overview of the global transcriptional profiling data for cytotrophoblasts of the smooth chorion in severe preeclampsia (sPE), non-infected preterm birth (nPTB) and the late second trimester of normal pregnancy (2nd Late). (A) Overlap of the differentially expressed genes in the three sample groups. Circle sizes are proportional to the number of differentially expressed genes. (B) Hierarchical clustering failed to completely separate the nPTB and Late 2nd trimester samples. In contrast, the sPE data clustered together.

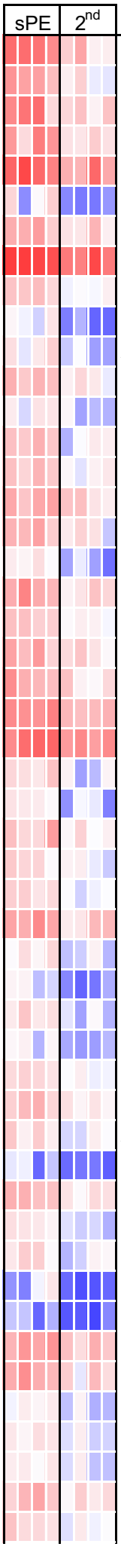

Symbol	Title	Δ
MT1H	metallothionein 1H	23
MT1G	metallothionein 1G	13
KRT24	keratin 24	11
CDSN	corneodesmosin	10
PAPPA	pregnancy-associated plasma protein A, pappalysin 1	8
OR2T5	olfactory receptor, family 2, subfamily T, member 5	6
RP11-78C3.1	novel transcript	5
PAPPA-AS1	PAPPA antisense RNA 1	5
KRT223P	keratin 223 pseudogene	5
TRAJ59	T cell receptor alpha joining 59 (non-functional)	4
ATP13A4-AS1	ATP13A4 antisense RNA 1	4
NRCAM	neuronal cell adhesion molecule	4
MTHFD1	formyltetrahydrofolate synthetase	4
SCEL	sciellin	4
PTPRQ	protein tyrosine phosphatase, receptor type, Q	4
RP11-407H12.8	novel transcript	4
GSTA3	glutathione S-transferase alpha 3	4
RNY4P23	RNA, Ro-associated Y4 pseudogene 23	4
T1560	T1560 protein	4
LOC103352541	uncharacterized LOC103352541	4
LOC100130476	uncharacterized LOC100130476	4
PRKXP1	protein kinase, X-linked, pseudogene 1	4
RNU12	RNA, U12 small nuclear	3
SNORD48	small nucleolar RNA, C/D box 48	3
RNU6-1065P	RNA, U6 small nuclear 1065, pseudogene	3
MIR3908	microRNA 3908	3
LOC255187	uncharacterized LOC255187	3
TTC21B-AS1	TTC21B antisense RNA 1	3
MIR630	microRNA 630	3
PLA2G4A	phospholipase A2, group IVA (cytosolic, calcium-dependent)	3
LOC101928461	uncharacterized LOC101928461	3
RNU5F-4P	RNA, U5F small nuclear 4, pseudogene	3
RP11-65J21.1	novel transcript	3
LPAL2	lipoprotein, Lp(a)-like 2, pseudogene	3
SNORA6	small nucleolar RNA, H/ACA box 6	3
DNAH11	dynein, axonemal, heavy chain 11	3
AQP9	aquaporin 9	3
IL13RA2	interleukin 13 receptor, alpha 2	3
TGFBR3L	transforming growth factor, beta receptor III-like	3
LINC01338	long intergenic non-protein coding RNA 1338	3
LINC00330	long intergenic non-protein coding RNA 330	3
RNU6-732P	RNA, U6 small nuclear 732, pseudogene	3
FCGR1C	Fc fragment of IgG, high affinity Ic, receptor (CD64), pseudogene	3
SERPINA3	serpin peptidase inhibitor, clade A (alpha-1 antiproteinase, antitrypsin), member 3	3
KDR	kinase insert domain receptor (a type III receptor tyrosine kinase)	3
IGHD2-8	immunoglobulin heavy diversity 2-8	3
ICA1L	islet cell autoantigen 1,69kDa-like	3
RNA5SP444	RNA, 5S ribosomal pseudogene 444	3
RP11-458D21.1	novel transcript	3
SMAD4	SMAD family member 4	3

sPE	2nd	Symbol	Title	Δ
		HAS2	hyaluronan synthase 2	3
		RN7SKP260	RNA, 7SK small nuclear pseudogene 260	3
		RNU4-76P	RNA, U4 small nuclear 76, pseudogene	3
		RP11-246K15.1	novel transcript	3
		SORBS1	sorbin and SH3 domain containing 1	3
		ARG1	arginase 1	3
		FBXO9	F-box protein 9	3
		RNU6-540P	RNA, U6 small nuclear 540, pseudogene	3
		SCARNA17	small Cajal body-specific RNA 17	3
		LOC101927483	uncharacterized LOC101927483	3
		CSH1	chorionic somatomammotropin hormone 1	3
		POTEF	POTE ankyrin domain family, member F	3
		MUM1L1	melanoma associated antigen (mutated) 1-like 1	2
		RNF185-AS1	RNF185 antisense RNA 1	2
		RNU5B-4P	RNA, U5B small nuclear 4, pseudogene	2
		LL0XNC01-237H	putative novel transcipt	2
		RNU6-453P	RNA, U6 small nuclear 453, pseudogene	2
		RNU6-65P	RNA, U6 small nuclear 65, pseudogene	2
		RP11-347J14.8	putative novel transcript	2
		AC008440.10	putative novel transcript	2
		OR5M1	olfactory receptor, family 5, subfamily M, member 1	2
		RNU6-1043P	RNA, U6 small nuclear 1043, pseudogene	2
		RP11-459O1.2	putative novel transcript	2
		RNU7-80P	RNA, U7 small nuclear 80 pseudogene	2
		IPW	imprinted in Prader-Willi syndrome (non-protein coding)	2
		MIR4540	microRNA 4540	2
		RNU2-11P	RNA, U2 small nuclear 11, pseudogene	2
		RNU7-51P	RNA, U7 small nuclear 51 pseudogene	2
		RP11-875H7.1	novel transcript	2
		PPP1R3C	protein phosphatase 1, regulatory subunit 3C	2
		ANKFN1	ankyrin-repeat and fibronectin type III domain containing 1	2
		PROSP	protein S pseudogene (beta)	2
		SCEL-AS1	SCEL antisense RNA 1	2
		AC004878.2	novel transcript	2
		RNU12-2P	RNA, U12 small nuclear 2, pseudogene	2
		LOC102724050	uncharacterized LOC102724050	2
		MIR4307	microRNA 4307	2
		RNU6-919P	RNA, U6 small nuclear 919, pseudogene	2
		MKLN1-AS	MKLN1 antisense RNA	2
		LOC101926943	uncharacterized LOC101926943	2
		ATP13A4	ATPase type 13A4	2
		LOC102724077	uncharacterized LOC102724077	2
		OR1S1	olfactory receptor, family 1, subfamily S, member 1	2
		KRTAP6-2	keratin associated protein 6-2	2
		LOC730081	uncharacterized LOC730081	2
		FOXJ3	forkhead box J3	2
		CSH2	chorionic somatomammotropin hormone 2	2
		RP11-661A12.4	7SK RNA	2
		OR2T34	olfactory receptor, family 2, subfamily T, member 34	2
		VPS37D	vacuolar protein sorting 37 homolog D (S. cerevisiae)	2

sPE	2nd	Symbol	Title	Δ
		OSER1-AS1	OSER1 antisense RNA 1 (head to head)	2
		C7orf69	chromosome 7 open reading frame 69	2
		LRRC17	leucine rich repeat containing 17	2
		RNA5SP255	RNA, 5S ribosomal pseudogene 255	2
		RP11-111F5.3	putative novel transcript	2
		MIR3152	microRNA 3152	2
		RNU4ATAC5P	RNA, U4atac small nuclear 5, pseudogene	2
		MIR548B	microRNA 548b	2
		RNA5SP222	RNA, 5S ribosomal pseudogene 222	2
		LOC101927468	uncharacterized LOC101927468	2
		RNU6-1286P	RNA, U6 small nuclear 1286, pseudogene	2
		LINC01003	long intergenic non-protein coding RNA 1003	2
		SNORD32A	small nucleolar RNA, C/D box 32A	2
		RNU6-206P	RNA, U6 small nuclear 206, pseudogene	2
		IGIP	IgA-inducing protein	2
		MAMDC2	MAM domain containing 2	2
		RIMBP3B	RIMS binding protein 3B	2
		RNA5SP347	RNA, 5S ribosomal pseudogene 347	2
		UGCG	UDP-glucose ceramide glucosyltransferase	2
		ERICH2	glutamate-rich 2	2
		MXD1	MAX dimerization protein 1	2
		TCERG1L-AS1	TCERG1L antisense RNA 1	2
		AFF1	AF4/FMR2 family, member 1	2
		KIAA1377	KIAA1377	2
		PTGER3	prostaglandin E receptor 3 (subtype EP3)	2
		LOC102724763	uncharacterized LOC102724763	2
		RNU6-478P	RNA, U6 small nuclear 478, pseudogene	2
		WFIKKN1	WAP, follistatin/kazal, immunoglobulin, kunitz and netrin domain containing 1	2
		TGIF2LY	TGFB-induced factor homeobox 2-like, Y-linked	2
		C12orf55	chromosome 12 open reading frame 55	2
		FIRRE	firre intergenic repeating RNA element	2
		LINC00202-2	long intergenic non-protein coding RNA 202-2	2
		PPM1N	protein phosphatase, Mg2+/Mn2+ dependent, 1N (putative)	2
		RP11-408J6.1	novel transcript, intronic to SEMA6D	2
		NRG4	neuregulin 4	2
		RNA5SP90	RNA, 5S ribosomal pseudogene 90	2
		RNU4-80P	RNA, U4 small nuclear 80, pseudogene	2
		LOC100506746	uncharacterized LOC100506746	2
		SNORD37	small nucleolar RNA, C/D box 37	2
		CCDC18	coiled-coil domain containing 18	-2
		ESCO2	establishment of sister chromatid cohesion N-acetyltransferase 2	-2
		HIST1H4I	histone cluster 1, H4i	-2
		KRT17P2	keratin 17 pseudogene 2	-2
		MBOAT2	membrane bound O-acyltransferase domain containing 2	-2
		PTER	phosphotriesterase related	-2
		RP11-681L8.1	novel transcript, sense overlapping to STPG2	-2
		TSPAN15	tetraspanin 15	-2
		RP11-48B3.3	novel transcript	-2
		AC097721.2	novel transcript	-2
		ANXA8	annexin A8	-2

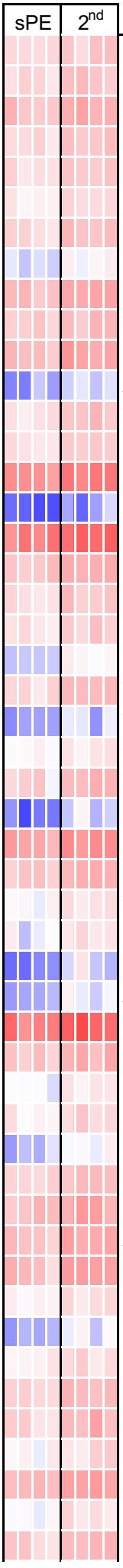

Symbol	Title	Δ
ISYNA1	inositol-3-phosphate synthase 1	-2
MFSD12	major facilitator superfamily domain containing 12	-2
NEDD4L	neural precursor cell expressed, developmentally down-regulated 4-like, E3 ubiquitin protein ligase	-2
SEPT6	septin 6	-2
SPNS2	spinster homolog 2 (Drosophila)	-2
CHEK1	checkpoint kinase 1	-2
RAB11FIP1	RAB11 family interacting protein 1 (class I)	-2
SIX4	SIX homeobox 4	-2
SPINT1	serine peptidase inhibitor, Kunitz type 1	-2
TIMM50	translocase of inner mitochondrial membrane 50 homolog (S. cerevisiae)	-2
SLC38A9	solute carrier family 38, member 9	-2
ATP6V0A4	ATPase, H+ transporting, lysosomal V0 subunit a4	-2
TMEM52B	transmembrane protein 52B	-2
COL4A5	collagen, type IV, alpha 5	-2
ERVH48-1	endogenous retrovirus group 48, member 1	-2
MIR301A	microRNA 301a	-2
MT-TT	mitochondrially encoded tRNA threonine	-2
GREB1L	growth regulation by estrogen in breast cancer-like	-2
BLNK	B-cell linker	-2
HCP5	HLA complex P5 (non-protein coding)	-2
LOC100288637	OTU deubiquitinase 7A pseudogene	-2
TGFB1	transforming growth factor, beta 1	-2
TPTE2	transmembrane phosphoinositide 3-phosphatase and tensin homolog 2	-2
TTC7B	tetratricopeptide repeat domain 7B	-2
INTS6	integrator complex subunit 6	-2
MIR1-2	microRNA 1-2	-2
RP2	retinitis pigmentosa 2 (X-linked recessive)	-2
SNORD10	small nucleolar RNA, C/D box 10	-2
WNT6	wingless-type MMTV integration site family, member 6	-2
RNU6-208P	RNA, U6 small nuclear 208, pseudogene	-2
RNU6-879P	RNA, U6 small nuclear 879, pseudogene	-2
AC093375.1	novel transcript	-2
ITGB6	integrin, beta 6	-2
LOC102725166	uncharacterized LOC102725166	-2
MYBL2	v-myb avian myeloblastosis viral oncogene homolog-like 2	-2
RNU6-1340P	RNA, U6 small nuclear 1340, pseudogene	-2
RP11-576N17.5	putative novel transcript	-2
SH2D4A	SH2 domain containing 4A	-2
SNORD50A	small nucleolar RNA, C/D box 50A	-2
ARL15	ADP-ribosylation factor-like 15	-2
PARP8	poly (ADP-ribose) polymerase family, member 8	-2
PLK1	polo-like kinase 1	-2
SLC15A2	solute carrier family 15 (oligopeptide transporter), member 2	-2
SLC22A11	solute carrier family 22 (organic anion/urate transporter), member 11	-2
DNMT1	DNA (cytosine-5-)-methyltransferase 1	-2
C5orf30	chromosome 5 open reading frame 30	-2
HAND1	heart and neural crest derivatives expressed 1	-2
LAMC2	laminin, gamma 2	-2
SIRPB2	signal-regulatory protein beta 2	-2
METTL7A	methyltransferase like 7A	-2

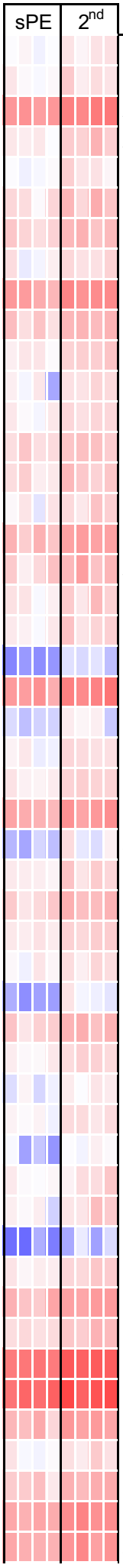

Symbol	Title	Δ
MIR619	microRNA 619	-2
SLC6A4	solute carrier family 6 (neurotransmitter transporter), member 4	-2
AC011558.5	novel transcript, antisense to CNN2	-2
AIM2	absent in melanoma 2	-2
CHI3L1	chitinase 3-like 1 (cartilage glycoprotein-39)	-2
HCST	hematopoietic cell signal transducer	-2
KIAA1217	KIAA1217	-2
LOC101928076	uncharacterized LOC101928076	-2
MAN1A1	mannosidase, alpha, class 1A, member 1	-2
MIR3916	microRNA 3916	-2
GINS1	GINS complex subunit 1 (Psf1 homolog)	-2
C6orf226	chromosome 6 open reading frame 226	-2
HJURP	Holliday junction recognition protein	-2
KIF4A	kinesin family member 4A	-2
LYPD3	LY6/PLAUR domain containing 3	-2
SIGLEC14	sialic acid binding Ig-like lectin 14	-2
FERMT1	fermitin family member 1	-2
ANKRD10-IT1	ANKRD10 intronic transcript 1 (non-protein coding)	-2
ITM2A	integral membrane protein 2A	-2
KIF13B	kinesin family member 13B	-2
RASGRP3	RAS guanyl releasing protein 3 (calcium and DAG-regulated)	-2
SMS	spermine synthase	-2
GBP1P1	guanylate binding protein 1, interferon-inducible pseudogene 1	-2
FFAR3	free fatty acid receptor 3	-2
GAS2L3	growth arrest-specific 2 like 3	-2
SORT1	sortilin 1	-2
ZNF66	zinc finger protein 66	-2
IRF1	interferon regulatory factor 1	-2
GEN1	GEN1 Holliday junction 5 flap endonuclease	-2
SPRY2	sprouty homolog 2 (Drosophila)	-2
FEZ1	fasciculation and elongation protein zeta 1 (zygin I)	-2
MND1	meiotic nuclear divisions 1 homolog (S. cerevisiae)	-2
ENAH	enabled homolog (Drosophila)	-2
RNU6-572P	RNA, U6 small nuclear 572, pseudogene	-2
TMEM194B	transmembrane protein 194B	-2
C5orf34	chromosome 5 open reading frame 34	-2
RP11-64D22.5	novel transcript	-2
CDH2	cadherin 2, type 1, N-cadherin (neuronal)	-2
GUCY1A3	guanylate cyclase 1, soluble, alpha 3	-2
INTS4L1	integrator complex subunit 4-like 1	-2
CDCA8	cell division cycle associated 8	-2
DUSP10	dual specificity phosphatase 10	-2
RP5-1087E8.3	putative novel transcript	-2
TPM4	tropomyosin 4	-2
GNG5P2	guanine nucleotide binding protein (G protein), gamma 5 pseudogene 2	-2
GBP3	guanylate binding protein 3	-2
PCDH10	protocadherin 10	-2
GPR115	G protein-coupled receptor 115	-2
BCAT1	branched chain amino-acid transaminase 1, cytosolic	-2
ZNF431	zinc finger protein 431	-2

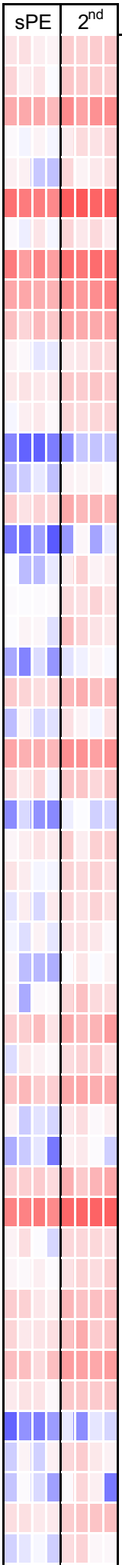

Symbol	Title	Δ
DTWD2	DTW domain containing 2	-2
CENPU	centromere protein U	-2
ANXA3	annexin A3	-2
SPC25	SPC25, NDC80 kinetochore complex component	-2
GGH	gamma-glutamyl hydrolase (conjugase, folylpolygammaglutamyl hydrolase)	-2
ITGA6	integrin, alpha 6	-2
RP11-184E9.1	novel transcript	-2
CAPN6	calpain 6	-2
KPNA2	karyopherin alpha 2 (RAG cohort 1, importin alpha 1)	-2
RFC3	replication factor C (activator 1) 3, 38kDa	-2
SH3RF2	SH3 domain containing ring finger 2	-2
RMI2	RecQ mediated genome instability 2	-2
IL32	interleukin 32	-2
RNU6-583P	RNA, U6 small nuclear 583, pseudogene	-2
RP11-108P20.4	novel transcript	-2
NUAK2	NUAK family, SNF1-like kinase, 2	-2
RNU6-1316P	RNA, U6 small nuclear 1316, pseudogene	-2
RNA5SP82	RNA, 5S ribosomal pseudogene 82	-2
TNF	tumor necrosis factor	-2
LOC101929579	uncharacterized LOC101929579	-2
ASF1B	anti-silencing function 1B histone chaperone	-2
CNN3	calponin 3, acidic	-2
CYP2D6	cytochrome P450, family 2, subfamily D, polypeptide 6	-2
SPOPL	speckle-type POZ protein-like	-2
POT1-AS1	POT1 antisense RNA 1	-2
GEMIN2	gem (nuclear organelle) associated protein 2	-2
REEP4	receptor accessory protein 4	-2
TRANK1	tetratricopeptide repeat and ankyrin repeat containing 1	-2
ICAM1	intercellular adhesion molecule 1	-2
LINC01036	long intergenic non-protein coding RNA 1036	-2
LOC101927841	uncharacterized LOC101927841	-2
ARHGAP11B	Rho GTPase activating protein 11B	-2
HCAR3	hydroxycarboxylic acid receptor 3	-2
SNAR-D	small ILF3/NF90-associated RNA D	-2
ECT2	epithelial cell transforming 2	-2
SPATA18	spermatogenesis associated 18	-2
ZNF554	zinc finger protein 554	-2
GLDC	glycine dehydrogenase (decarboxylating)	-2
SCCPDH	saccharopine dehydrogenase (putative)	-2
RNF128	ring finger protein 128, E3 ubiquitin protein ligase	-2
SLC44A3	solute carrier family 44, member 3	-2
DTL	denticleless E3 ubiquitin protein ligase homolog (Drosophila)	-2
RNU6-801P	RNA, U6 small nuclear 801, pseudogene	-2
CXCL2	chemokine (C-X-C motif) ligand 2	-2
ARHGAP23P1	Rho GTPase activating protein 23 pseudogene 1	-2
RP11-203H2.2	novel transcript	-2
MIR521-1	microRNA 521-1	-2
MIR3671	microRNA 3671	-2
MKI67	marker of proliferation Ki-67	-2
RPS3A	ribosomal protein S3A	-2

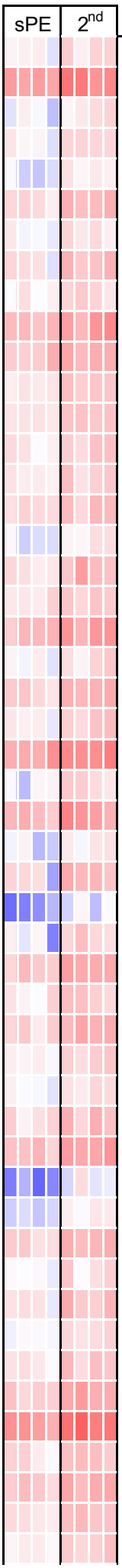

Symbol	Title	Δ
TK1	thymidine kinase 1, soluble	-2
KRT16P4	keratin 16 pseudogene 4	-2
LOC101927260	uncharacterized LOC101927260	-2
RP11-1166P10.1	Rho GTPase activating protein 23 (ARHGAP23) pseudogene	-2
KIF15	kinesin family member 15	-2
KIF23	kinesin family member 23	-2
STIL	SCL/TAL1 interrupting locus	-2
TTK	TTK protein kinase	-2
COBL	cordon-bleu WH2 repeat protein	-3
HIST2H2BA	histone cluster 2, H2ba (pseudogene)	-3
HMGA1	high mobility group AT-hook 1	-3
YBX3P1	Y box binding protein 3 pseudogene 1	-3
FANCD2	Fanconi anemia, complementation group D2	-3
TLR2	toll-like receptor 2	-3
CDH5	cadherin 5, type 2 (vascular endothelium)	-3
GATSL2	GATS protein-like 2	-3
FCGBP	Fc fragment of IgG binding protein	-3
RNU6-580P	RNA, U6 small nuclear 580, pseudogene	-3
TMEM63A	transmembrane protein 63A	-3
MIR622	microRNA 622	-3
TRDJ3	T cell receptor delta joining 3	-3
KIF20B	kinesin family member 20B	-3
FAM169A	family with sequence similarity 169, member A	-3
BTG2	BTG family, member 2	-3
TPTE	transmembrane phosphatase with tensin homology	-3
GBP1	guanylate binding protein 1, interferon-inducible	-3
CLSPN	claspin	-3
MIR103B2	microRNA 103b-2	-3
RNU6-971P	RNA, U6 small nuclear 971, pseudogene	-3
RNU6-151P	RNA, U6 small nuclear 151, pseudogene	-3
ITGB4	integrin, beta 4	-3
KRT17P1	keratin 17 pseudogene 1	-3
CDCP1	CUB domain containing protein 1	-3
PBK	PDZ binding kinase	-3
KIAA0101	KIAA0101	-3
TAGLN	transgelin	-3
FOXO4	forkhead box O4	-3
RNU6-850P	RNA, U6 small nuclear 850, pseudogene	-3
RAD51	RAD51 recombinase	-3
CDKN3	cyclin-dependent kinase inhibitor 3	-3
RP11-517O13.1	novel transcript, antisense to TIMM9	-3
ATP6V1C2	ATPase, H+ transporting, lysosomal 42kDa, V1 subunit C2	-3
CEP55	centrosomal protein 55kDa	-3
PRR11	proline rich 11	-3
TP63	tumor protein p63	-3
CD47	CD47 molecule	-3
EFNB2	ephrin-B2	-3
ARHGAP18	Rho GTPase activating protein 18	-3
PRC1	protein regulator of cytokinesis 1	-3
P2RY6	pyrimidinergic receptor P2Y, G-protein coupled, 6	-3

sPE	2nd	Symbol	Title	Δ
		CKAP2	cytoskeleton associated protein 2	-3
		CKS2	CDC28 protein kinase regulatory subunit 2	-3
		KRAS	Kirsten rat sarcoma viral oncogene homolog	-3
		RNA5SP282	RNA, 5S ribosomal pseudogene 282	-3
		CCDC81	coiled-coil domain containing 81	-3
		BLM	Bloom syndrome, RecQ helicase-like	-3
		CKAP2L	cytoskeleton associated protein 2-like	-3
		HSD17B1	hydroxysteroid (17-beta) dehydrogenase 1	-3
		ANKRD36BP2	ankyrin repeat domain 36B pseudogene 2	-3
		KRT18P15	keratin 18 pseudogene 15	-3
		SGOL1	shugoshin-like 1 (S. pombe)	-3
		SNAR-C2	small ILF3/NF90-associated RNA C2	-3
		RNU6-226P	RNA, U6 small nuclear 226, pseudogene	-3
		MIR15B	microRNA 15b	-3
		LOC102724842	uncharacterized LOC102724842	-3
		AC078883.4	novel transcript	-3
		RNU6-531P	RNA, U6 small nuclear 531, pseudogene	-3
		RP11-49I4.3	novel transcript	-3
		EXO1	exonuclease 1	-3
		MIR520E	microRNA 520e	-3
		KRT23	keratin 23 (histone deacetylase inducible)	-3
		KDM4B	lysine (K)-specific demethylase 4B	-3
		COL15A1	collagen, type XV, alpha 1	-3
		RNA5SP330	RNA, 5S ribosomal pseudogene 330	-3
		RP11-524H19.2	putative novel transcript	-3
		LOC101927700	uncharacterized LOC101927700	-3
		AGL	amylo-alpha-1, 6-glucosidase, 4-alpha-glucanotransferase	-3
		CCL4	chemokine (C-C motif) ligand 4	-3
		RNU6-83P	RNA, U6 small nuclear 83, pseudogene	-3
		CENPF	centromere protein F, 350/400kDa	-3
		SLC7A6	solute carrier family 7 (amino acid transporter light chain, y+L system), member 6	-3
		MIR498	microRNA 498	-3
		KRT18P49	keratin 18 pseudogene 49	-3
		SNORA53	small nucleolar RNA, H/ACA box 53	-3
		CDCA2	cell division cycle associated 2	-3
		GPR137B	G protein-coupled receptor 137B	-3
		LOC101927202	uncharacterized LOC101927202	-3
		MYH10	myosin, heavy chain 10, non-muscle	-3
		SMPDL3A	sphingomyelin phosphodiesterase, acid-like 3A	-3
		SFN	stratifin	-3
		NUF2	NUF2, NDC80 kinetochore complex component	-3
		NRN1L	neuritin 1-like	-3
		LAMB4	laminin, beta 4	-3
		OCLN	occludin	-3
		PLAU	plasminogen activator, urokinase	-3
		CACNG4	calcium channel, voltage-dependent, gamma subunit 4	-3
		MCM6	minichromosome maintenance complex component 6	-3
		RNU7-43P	RNA, U7 small nuclear 43 pseudogene	-3
		PGAP1	post-GPI attachment to proteins 1	-3
		AGR2	anterior gradient 2	-3

sPE	2nd	Symbol	Title	Δ
		LBR	lamin B receptor	-3
		KRT18P54	keratin 18 pseudogene 54	-3
		CSF3R	colony stimulating factor 3 receptor (granulocyte)	-3
		KIAA1524	KIAA1524	-3
		RRM2	ribonucleotide reductase M2	-3
		HNRNPA1P33	heterogeneous nuclear ribonucleoprotein A1 pseudogene 33	-3
		RBMS3	RNA binding motif, single stranded interacting protein 3	-3
		PLK4	polo-like kinase 4	-3
		MIR548AL	microRNA 548al	-3
		ORC6	origin recognition complex, subunit 6	-3
		RNU6-780P	RNA, U6 small nuclear 780, pseudogene	-3
		CASC5	cancer susceptibility candidate 5	-3
		BIRC5	baculoviral IAP repeat containing 5	-3
		LMNB1	lamin B1	-3
		RNU6-803P	RNA, U6 small nuclear 803, pseudogene	-3
		RN7SKP42	RNA, 7SK small nuclear pseudogene 42	-3
		FGFR2	fibroblast growth factor receptor 2	-3
		ZDHHC2	zinc finger, DHHC-type containing 2	-3
		KRT18P10	keratin 18 pseudogene 10	-3
		RNU6-560P	RNA, U6 small nuclear 560, pseudogene	-3
		CENPK	centromere protein K	-3
		AFAP1L2	actin filament associated protein 1-like 2	-3
		SNORD35A	small nucleolar RNA, C/D box 35A	-3
		NLRP2	NLR family, pyrin domain containing 2	-3
		SLC43A2	solute carrier family 43 (amino acid system L transporter), member 2	-3
		NLRP7	NLR family, pyrin domain containing 7	-3
		RNA5SP474	RNA, 5S ribosomal pseudogene 474	-3
		TMC7	transmembrane channel-like 7	-3
		TPX2	TPX2, microtubule-associated	-3
		AREG	amphiregulin	-3
		CCNA2	cyclin A2	-3
		CCNB2	cyclin B2	-3
		EPCAM	epithelial cell adhesion molecule	-3
		CENPH	centromere protein H	-3
		CLU	clusterin	-3
		DRAM1	DNA-damage regulated autophagy modulator 1	-3
		GPR82	G protein-coupled receptor 82	-3
		SLC7A5	solute carrier family 7 (amino acid transporter light chain, L system), member 5	-3
		HELLS	helicase, lymphoid-specific	-3
		CST6	cystatin E/M	-3
		RP11-1M18.1	novel transcript	-3
		KIF11	kinesin family member 11	-3
		HAPLN1	hyaluronan and proteoglycan link protein 1	-3
		MEST	mesoderm specific transcript	-3
		RNU6-308P	RNA, U6 small nuclear 308, pseudogene	-3
		PLS1	plastin 1	-3
		CCNB1	cyclin B1	-4
		PVRL2	poliovirus receptor-related 2 (herpesvirus entry mediator B)	-4
		GPR37	G protein-coupled receptor 37 (endothelin receptor type B-like)	-4
		SNORD16	small nucleolar RNA, C/D box 16	-4

sPE	2nd	Symbol	Title	Δ
		XAGE3	X antigen family, member 3	-4
		TOP2A	topoisomerase (DNA) II alpha 170kDa	-4
		CD274	CD274 molecule	-4
		RNU6-79P	RNA, U6 small nuclear 79, pseudogene	-4
		FAR2P2	fatty acyl CoA reductase 2 pseudogene 2	-4
		RAD51AP1	RAD51 associated protein 1	-4
		TINAGL1	tubulointerstitial nephritis antigen-like 1	-4
		COL1A2	collagen, type I, alpha 2	-4
		DIAPH3	diaphanous-related formin 3	-4
		OLR1	oxidized low density lipoprotein (lectin-like) receptor 1	-4
		DDAH1	dimethylarginine dimethylaminohydrolase 1	-4
		HSD17B2	hydroxysteroid (17-beta) dehydrogenase 2	-4
		MIR7641-2	microRNA 7641-2	-4
		DSCC1	DNA replication and sister chromatid cohesion 1	-4
		COL3A1	collagen, type III, alpha 1	-4
		RNU6-223P	RNA, U6 small nuclear 223, pseudogene	-4
		TP53INP1	tumor protein p53 inducible nuclear protein 1	-4
		AC106053.1	novel transcript	-4
		SERPINF1	serpin peptidase inhibitor, clade F1	-4
		RNU6-623P	RNA, U6 small nuclear 623, pseudogene	-4
		BUB1	BUB1 mitotic checkpoint serine/threonine kinase	-4
		KIF14	kinesin family member 14	-4
		PDIA6	protein disulfide isomerase family A, member 6	-4
		RNU6-387P	RNA, U6 small nuclear 387, pseudogene	-4
		TYMS	thymidylate synthetase	-4
		RNU6-1195P	RNA, U6 small nuclear 1195, pseudogene	-4
		ARHGAP11A	Rho GTPase activating protein 11A	-4
		DLGAP5	discs, large (Drosophila) homolog-associated protein 5	-4
		CTD-2306M5.1	novel transcript	-4
		MIR218-1	microRNA 218-1	-4
		SHCBP1	SHC SH2-domain binding protein 1	-4
		CENPE	centromere protein E, 312kDa	-4
		HIST1H3E	histone cluster 1, H3e	-4
		C10orf55	chromosome 10 open reading frame 55	-4
		MELK	maternal embryonic leucine zipper kinase	-4
		SNORD75	small nucleolar RNA, C/D box 75	-4
		FMOD	fibromodulin	-4
		RNU6-736P	RNA, U6 small nuclear 736, pseudogene	-4
		PABPC4L	poly(A) binding protein, cytoplasmic 4-like	-4
		LINC01237	long intergenic non-protein coding RNA 1237	-4
		RNU6-606P	RNA, U6 small nuclear 606, pseudogene	-4
		GBP2	guanylate binding protein 2, interferon-inducible	-4
		AP001615.9	putative novel transcript	-4
		CDC6	cell division cycle 6	-4
		SKA3	spindle and kinetochore associated complex subunit 3	-4
		NCAPG	non-SMC condensin I complex, subunit G	-4
		EPPK1	epiplakin 1	-4
		TSPAN2	tetraspanin 2	-4
		RNU6-375P	RNA, U6 small nuclear 375, pseudogene	-4
		SNORD2	small nucleolar RNA, C/D box 2	-4

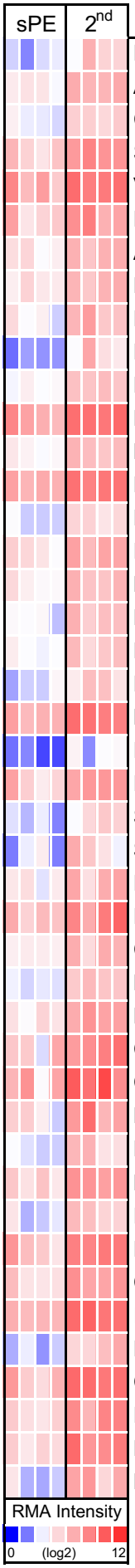

Symbol	Title	Δ
RNU6-1318P	RNA, U6 small nuclear 1318, pseudogene	-5
ASPM	asp (abnormal spindle) homolog, microcephaly associated (Drosophila)	-5
CDK1	cyclin-dependent kinase 1	-5
SIGLEC6	sialic acid binding Ig-like lectin 6	-5
VIT	vitrin	-5
RNU6-1170P	RNA, U6 small nuclear 1170, pseudogene	-5
AIM1	absent in melanoma 1	-5
NUSAP1	nucleolar and spindle associated protein 1	-5
RNU6-1188P	RNA, U6 small nuclear 1188, pseudogene	-5
RNA5SP88	RNA, 5S ribosomal pseudogene 88	-5
PMAIP1	phorbol-12-myristate-13-acetate-induced protein 1	-5
NRK	Nik related kinase	-5
BRIP1	BRCA1 interacting protein C-terminal helicase 1	-5
PAGE4	P antigen family, member 4 (prostate associated)	-5
RP4-694A7.2	putative novel transcript	-5
HMMR	hyaluronan-mediated motility receptor (RHAMM)	-5
KIF18A	kinesin family member 18A	-5
NDC80	NDC80 kinetochore complex component	-5
DEPDC1	DEP domain containing 1	-5
RNU4-54P	RNA, U4 small nuclear 54, pseudogene	-5
KRT17	keratin 17	-5
HIST1H3B	histone cluster 1, H3b	-5
HGF	hepatocyte growth factor (hepapoietin A; scatter factor)	-6
SUCNR1	succinate receptor 1	-6
SNORD111	small nucleolar RNA, C/D box 111	-6
HIST1H3F	histone cluster 1, H3f	-6
HIST1H3I	histone cluster 1, H3i	-6
CLDN6	claudin 6	-6
LRP2	low density lipoprotein receptor-related protein 2	-6
MIR205HG	MIR205 host gene (non-protein coding)	-6
CCL2	chemokine (C-C motif) ligand 2	-6
CXCL10	chemokine (C-X-C motif) ligand 10	-6
MIR1323	microRNA 1323	-6
PRSS12	protease, serine, 12 (neurotrypsin, motopsin)	-6
LPHN3	latrophilin 3	-6
F5	coagulation factor V (proaccelerin, labile factor)	-7
EGFL6	EGF-like-domain, multiple 6	-7
CDO1	cysteine dioxygenase type 1	-7
ITGA2	integrin, alpha 2 (CD49B, alpha 2 subunit of VLA-2 receptor)	-8
RNU6-1330P	RNA, U6 small nuclear 1330, pseudogene	-8
CD24	CD24 molecule	-10
HIST1H2AM	histone cluster 1, H2am	-10
NPPB	natriuretic peptide B	-11
MIR515-1	microRNA 515-1	-26

Supplemental Figure 4. Global gene expression profiles of schCTBs isolated by laser capture microdissection from the fetal membranes: severe preeclampsia (sPE) as compared to the late second trimester of normal pregnancy (2^{nd}) (n=4/group). The heatmap lists genes that were differentially expressed by 2-fold or greater.

nPTB	2nd	Symbol	Title	Δ
		SPINK1	serine peptidase inhibitor, Kazal type 1	12
		HLA-DRB1	major histocompatibility complex, class II, DR beta 1	12
		RNU6-1154P	RNA, U6 small nuclear 1154, pseudogene	10
		RNU6-638P	RNA, U6 small nuclear 638, pseudogene	7
		BMP2	bone morphogenetic protein 2	7
		KLHL22-IT1	KLHL22 intronic transcript 1 (non-protein coding)	6
		HK2	hexokinase 2	5
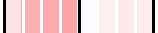		LRRC15	leucine rich repeat containing 15	5
		RNU1-124P	RNA, U1 small nuclear 124, pseudogene	5
		PPP1R3C	protein phosphatase 1, regulatory subunit 3C	5
		MIR302A	microRNA 302a	5
		RP11-407H12.8	novel transcript	4
		SNORA29	small nucleolar RNA, H/ACA box 29	4
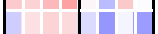		RNU6-540P	RNA, U6 small nuclear 540, pseudogene	4
		RNU6-1014P	RNA, U6 small nuclear 1014, pseudogene	4
		RNU5F-4P	RNA, U5F small nuclear 4, pseudogene	4
		SNORD59A	small nucleolar RNA, C/D box 59A	4
		SCEL	sciellin	4
		ATP13A4	ATPase type 13A4	3
		AC008269.2	putative novel transcript	3
		CES1	carboxylesterase 1	3
		GJB3	gap junction protein, beta 3, 31kDa	3
		LOC101928461	uncharacterized LOC101928461	3
		DDIT4	DNA-damage-inducible transcript 4	3
		RP11-48B3.5	novel transcript, antisense to ZBTB10	3
		RP11-138H8.2	novel transcript	3
		HRASLS2	HRAS-like suppressor 2	3
		SNORD48	small nucleolar RNA, C/D box 48	3
		FCGR1C	Fc fragment of IgG, high affinity Ic, receptor (CD64), pseudogene	3
		SNORD68	small nucleolar RNA, C/D box 68	3
		MIR1204	microRNA 1204	3
		SERPINA3	serpin peptidase inhibitor, clade A (alpha-1 antiproteinase, antitrypsin), member 3	3
		RNU7-9P	RNA, U7 small nuclear 9 pseudogene	3
		RNU4-21P	RNA, U4 small nuclear 21, pseudogene	3
		RNU6-249P	RNA, U6 small nuclear 249, pseudogene	3
		FAM86EP	family with sequence similarity 86, member A pseudogene	3
		LINC00152	long intergenic non-protein coding RNA 152 (LOC101930489)	3
		SNORD33	small nucleolar RNA, C/D box 33	3
		RNA5SP155	RNA, 5S ribosomal pseudogene 155	3
		KLF9	Kruppel-like factor 9	3
		RNU7-62P	RNA, U7 small nuclear 62 pseudogene	3
		RNU4-76P	RNA, U4 small nuclear 76, pseudogene	3
		LOC101930489	uncharacterized LOC101930489	3
		ADM	adrenomedullin	3
		GFPT2	glutamine-fructose-6-phosphate transaminase 2	3
		RP11-458D21.1	novel transcript	3
		MT1M	metallothionein 1M	3
		SNORD61	small nucleolar RNA, C/D box 61	3
		GK-AS1	GK antisense RNA 1	3
		C15orf48	chromosome 15 open reading frame 48	3

nPTB	2nd	Symbol	Title	Δ
		RNU7-80P	RNA, U7 small nuclear 80 pseudogene	3
		IRS2	insulin receptor substrate 2	3
		RNA5SP468	RNA, 5S ribosomal pseudogene 468	3
		ZNF812	zinc finger protein 812	2
		OR10G7	olfactory receptor, family 10, subfamily G, member 7	2
		SV2B	synaptic vesicle glycoprotein 2B	2
		SRGAP2	SLIT-ROBO Rho GTPase activating protein 2	2
		PER1	period circadian clock 1	2
		RNU7-26P	RNA, U7 small nuclear 26 pseudogene	2
		RNU6-1230P	RNA, U6 small nuclear 1230, pseudogene	2
		KRTAP6-2	keratin associated protein 6-2	2
		RNU7-51P	RNA, U7 small nuclear 51 pseudogene	2
		RNU7-136P	RNA, U7 small nuclear 136 pseudogene	2
		RSF1-IT1	RSF1 intronic transcript 1 (non-protein coding)	2
		DUSP5	dual specificity phosphatase 5	2
		RP11-33I11.2	putative novel transcript	2
		MMP10	matrix metallopeptidase 10 (stromelysin 2)	2
		RP11-10J5.1	putative novel transcript	2
		RP11-812E19.9	novel gene similar to an immunoglobulin heavy variable 3/OR16 gene	2
		RNA5SP287	RNA, 5S ribosomal pseudogene 287	2
		RP11-38L15.2	novel transcript	2
		RNA5SP255	RNA, 5S ribosomal pseudogene 255	2
		IL23A	interleukin 23, alpha subunit p19	2
		SNORA15	small nucleolar RNA, H/ACA box 15	2
		RP11-549L6.3	putative novel transcript	2
		CELSR3-AS1	CELSR3 antisense RNA 1 (head to head)	2
		RNY3P8	RNA, Ro-associated Y3 pseudogene 8	2
		AC068491.2	putative novel transcript	2
		TRAJ14	T cell receptor alpha joining 14	2
		APOOP5	apolipoprotein O pseudogene 5	2
		IRF2BP2	interferon regulatory factor 2 binding protein 2	2
		RN7SKP140	RNA, 7SK small nuclear pseudogene 140	2
		CTD-2501M5.1	novel transcript	2
		RP11-212I21.2	novel transcript	2
		RNA5SP489	RNA, 5S ribosomal pseudogene 489	2
		MIR378F	microRNA 378f	2
		RNA5SP185	RNA, 5S ribosomal pseudogene 185	2
		DLEU2L	deleted in lymphocytic leukemia 2-like	2
		INTS4	integrator complex subunit 4	2
		LOC101927468	uncharacterized LOC101927468	2
		B3GALTL	beta 1,3-galactosyltransferase-like	2
		MIR1537	microRNA 1537	2
		CTB-4E7.1	novel transcript	2
		GEM	GTP binding protein overexpressed in skeletal muscle	2
		MIR551A	microRNA 551a	2
		RNU2-71P	RNA, U2 small nuclear 71, pseudogene	2
		RN7SKP142	RNA, 7SK small nuclear pseudogene 142	2
		RNA5SP460	RNA, 5S ribosomal pseudogene 460	2
		RNU4-41P	RNA, U4 small nuclear 41, pseudogene	2
		RNU4ATAC10P	RNA, U4atac small nuclear 10, pseudogene	2

nPTB	2nd	Symbol	Title	Δ
		VTRNA1-1	vault RNA 1-1	2
		MIR365A	microRNA 365a	2
		MIR4463	microRNA 4463	2
		RNU7-59P	RNA, U7 small nuclear 59 pseudogene	2
		RP11-400L8.2	novel transcript	2
		KIF15	kinesin family member 15	-2
		HIST1H2BE	histone cluster 1, H2be	-2
		LOC102723627	uncharacterized LOC102723627	-2
		SLC40A1	solute carrier family 40 (iron-regulated transporter), member 1	-2
		TIA1	TIA1 cytotoxic granule-associated RNA binding protein	-2
		CPNE2	copine II	-2
		WDHD1	WD repeat and HMG-box DNA binding protein 1	-2
		FERMT1	fermitin family member 1	-2
		SPC25	SPC25, NDC80 kinetochore complex component	-2
		PLK4	polo-like kinase 4	-2
		KIAA1549	KIAA1549	-2
		LRRC28	leucine rich repeat containing 28	-2
		AP000704.5	putative novel transcript	-2
		COLEC12	collectin sub-family member 12	-2
		DNA2	DNA replication helicase/nuclease 2	-2
		IGSF10	immunoglobulin superfamily, member 10	-2
		LGSN	lengsin, lens protein with glutamine synthetase domain	-2
		LOC101928054	uncharacterized LOC101928054	-2
		ZNF43	zinc finger protein 43	-2
		CD274	CD274 molecule	-2
		CDK1	cyclin-dependent kinase 1	-2
		ACPP	acid phosphatase, prostate	-2
		CTA-398F10.2	novel transcript	-2
		FOCAD	focadhesin	-2
		MTRNR2L6	MT-RNR2-like 6	-2
		GREB1L	growth regulation by estrogen in breast cancer-like	-2
		CDH2	cadherin 2, type 1, N-cadherin (neuronal)	-2
		LOC101927700	uncharacterized LOC101927700	-2
		CS	citrate synthase	-2
		LOC100287834	uncharacterized LOC100287834	-2
		ZNF229	zinc finger protein 229	-2
		GEN1	GEN1 Holliday junction 5 flap endonuclease	-2
		TGFB3	transforming growth factor, beta 3	-2
		LINC01355	long intergenic non-protein coding RNA 1355	-2
		RN7SKP163	RNA, 7SK small nuclear pseudogene 163	-2
		RP3-368A4.5	novel transcript, sense intronic FTX	-2
		SLC44A2	solute carrier family 44 (choline transporter), member 2	-2
		TMEM117	transmembrane protein 117	-2
		CD24	CD24 molecule	-2
		AC016644.1	novel transcript	-2
		RP11-710F7.2	novel transcript	-2
		SYDE2	synapse defective 1, Rho GTPase, homolog 2 (C. elegans)	-2
		LOXL1	lysyl oxidase-like 1	-2
		TNFRSF21	tumor necrosis factor receptor superfamily, member 21	-2
		TYMS	thymidylate synthetase	-2

nPTB	2nd	Symbol	Title	Δ
		BST1	bone marrow stromal cell antigen 1	-2
		SMG8	SMG8 nonsense mediated mRNA decay factor	-2
		RNU6-858P	RNA, U6 small nuclear 858, pseudogene	-2
		GINS2	GINS complex subunit 2 (Psf2 homolog)	-2
		LOC400541	uncharacterized LOC400541	-2
		SLC39A11	solute carrier family 39, member 11	-2
		DNMT1	DNA (cytosine-5-)-methyltransferase 1	-2
		AP001615.9	putative novel transcript	-2
		AC092597.3	novel transcript	-2
		ZNF554	zinc finger protein 554	-2
		ATP6V1C2	ATPase, H+ transporting, lysosomal 42kDa, V1 subunit C2	-2
		SESN3	sestrin 3	-2
		DTWD2	DTW domain containing 2	-2
		RRM2	ribonucleotide reductase M2	-2
		KGFLP2	keratinocyte growth factor-like protein 2	-2
		PPP1R9A	protein phosphatase 1, regulatory subunit 9A	-2
		DGCR11	DiGeorge syndrome critical region gene 11 (non-protein coding)	-2
		EXO1	exonuclease 1	-2
		AGAP6	ArfGAP with GTPase domain, ankyrin repeat and PH domain 6	-2
		DTL	denticleless E3 ubiquitin protein ligase homolog (Drosophila)	-2
		EFNB2	ephrin-B2	-2
		CASP6	caspase 6, apoptosis-related cysteine peptidase	-2
		COL14A1	collagen, type XIV, alpha 1	-2
		LOC283299	uncharacterized LOC283299	-2
		LOC101929579	uncharacterized LOC101929579	-2
		COL1A1	collagen, type I, alpha 1	-2
		ZNF329	zinc finger protein 329	-2
		NUF2	NUF2, NDC80 kinetochore complex component	-2
		PHC1	polyhomeotic homolog 1 (Drosophila)	-2
		GNG5P2	guanine nucleotide binding protein (G protein), gamma 5 pseudogene 2	-2
		TPX2	TPX2, microtubule-associated	-2
		ASH1L-IT1	ASH1L intronic transcript 1 (non-protein coding)	-2
		ARHGAP11B	Rho GTPase activating protein 11B	-2
		KDM4B	lysine (K)-specific demethylase 4B	-2
		TUSC3	tumor suppressor candidate 3	-2
		RAB11FIP4	RAB11 family interacting protein 4 (class II)	-2
		KIF18A	kinesin family member 18A	-2
		XRCC2	X-ray repair complementing defective repair in Chinese hamster cells 2	-2
		RAB9BP1	RAB9B, member RAS oncogene family pseudogene 1	-2
		GPR126	G protein-coupled receptor 126	-2
		SH3RF2	SH3 domain containing ring finger 2	-2
		DIAPH3	diaphanous-related formin 3	-2
		FZD3	frizzled class receptor 3	-2
		PPP2R3A	protein phosphatase 2, regulatory subunit B, alpha	-2
		FANCD2	Fanconi anemia, complementation group D2	-2
		CCNB1	cyclin B1	-2
		DDAH1	dimethylarginine dimethylaminohydrolase 1	-2
		RNU6-208P	RNA, U6 small nuclear 208, pseudogene	-2
		ATP10D	ATPase, class V, type 10D	-2
		RNU2-58P	RNA, U2 small nuclear 58, pseudogene	-2

nPTB	2nd	Symbol	Title	Δ
		ORC6	origin recognition complex, subunit 6	-2
		SOX4	SRY (sex determining region Y)-box 4	-2
		SLC38A9	solute carrier family 38, member 9	-2
		ANKRD10-IT1	ANKRD10 intronic transcript 1 (non-protein coding)	-2
		GPR82	G protein-coupled receptor 82	-2
		BUB1	BUB1 mitotic checkpoint serine/threonine kinase	-2
		PGAP1	post-GPI attachment to proteins 1	-2
		AFAP1L2	actin filament associated protein 1-like 2	-2
		MYO6	myosin VI	-2
		SUSD1	sushi domain containing 1	-2
		CYP2D6	cytochrome P450, family 2, subfamily D, polypeptide 6	-2
		LMNB1	lamin B1	-2
		ZNF99	zinc finger protein 99	-2
		SPOPL	speckle-type POZ protein-like	-2
		RP11-48B3.3	novel transcript	-2
		TMEM254-AS1	TMEM254 antisense RNA 1	-2
		SLC23A2	solute carrier family 23 (ascorbic acid transporter), member 2	-2
		COL15A1	collagen, type XV, alpha 1	-2
		NLRP7	NLR family, pyrin domain containing 7	-2
		CD200R1	CD200 receptor 1	-2
		RP11-574K11.5	putative novel transcript	-2
		TTC7B	tetratricopeptide repeat domain 7B	-2
		PBX1	pre-B-cell leukemia homeobox 1	-2
		CD36	CD36 molecule (thrombospondin receptor)	-2
		CEP55	centrosomal protein 55kDa	-2
		BRCA2	breast cancer 2, early onset	-2
		LOC441601	septin 7 pseudogene	-2
		MIR15B	microRNA 15b	-2
		PCDH10	protocadherin 10	-2
		RNU6-1330P	RNA, U6 small nuclear 1330, pseudogene	-3
		RNU6-879P	RNA, U6 small nuclear 879, pseudogene	-3
		RNU6-850P	RNA, U6 small nuclear 850, pseudogene	-3
		RP4-778K6.3	putative novel transcript	-3
		AC004160.4	putative novel transcript	-3
		ZNF594	zinc finger protein 594	-3
		NBPF1	neuroblastoma breakpoint family, member 1	-3
		RNU6-801P	RNA, U6 small nuclear 801, pseudogene	-3
		F2RL1	coagulation factor II (thrombin) receptor-like 1	-3
		LOC643072	uncharacterized LOC643072	-3
		HYAL4	hyaluronoglucosaminidase 4	-3
		ARHGAP23P1	Rho GTPase activating protein 23 pseudogene 1	-3
		C15orf41	chromosome 15 open reading frame 41	-3
		AC097721.2	novel transcript	-3
		CABLES1	Cdk5 and Abl enzyme substrate 1	-3
		RNA5SP282	RNA, 5S ribosomal pseudogene 282	-3
		HSD17B2	hydroxysteroid (17-beta) dehydrogenase 2	-3
		CCNB2	cyclin B2	-3
		PDIA6	protein disulfide isomerase family A, member 6	-3
		RN7SKP116	RNA, 7SK small nuclear pseudogene 116	-3
		CDH5	cadherin 5, type 2 (vascular endothelium)	-3

nPTB	2nd	Symbol	Title	Δ
		TFPI2	tissue factor pathway inhibitor 2	-3
		LILRA6	leukocyte immunoglobulin-like receptor, subfamily A (with TM domain), member 6	-3
		ZNF681	zinc finger protein 681	-3
		RNU4-16P	RNA, U4 small nuclear 16, pseudogene	-3
		CENPU	centromere protein U	-3
		GSG2	germ cell associated 2 (haspin)	-3
		LINC00308	long intergenic non-protein coding RNA 308	-3
		RNU6-83P	RNA, U6 small nuclear 83, pseudogene	-3
		DPP4	dipeptidyl-peptidase 4	-3
		SNORD113-1	small nucleolar RNA, C/D box 113-1	-3
		XAGE3	X antigen family, member 3	-3
		RNU6-1188P	RNA, U6 small nuclear 1188, pseudogene	-3
		RP11-49I4.3	novel transcript	-3
		MXRA5	matrix-remodelling associated 5	-3
		GUCY1A3	guanylate cyclase 1, soluble, alpha 3	-3
		PSG9	pregnancy specific beta-1-glycoprotein 9	-3
		RNA5SP424	RNA, 5S ribosomal pseudogene 424	-3
		CTD-2562J17.7	novel trancript	-3
		CCDC81	coiled-coil domain containing 81	-3
		KIAA0101	KIAA0101	-3
		ASPN	asporin	-3
		LOC101929607	uncharacterized LOC101929607	-3
		LOC644919	uncharacterized LOC644919	-3
		RP1-69D17.3	putative novel transcript	-3
		NDC80	NDC80 kinetochore complex component	-3
		DSCC1	DNA replication and sister chromatid cohesion 1	-3
		RP11-337C18.8	novel transcript	-3
		ARHGAP11A	Rho GTPase activating protein 11A	-3
		SHCBP1	SHC SH2-domain binding protein 1	-3
		LPHN3	latrophilin 3	-3
		GPR115	G protein-coupled receptor 115	-3
		NUSAP1	nucleolar and spindle associated protein 1	-3
		RNU6-512P	RNA, U6 small nuclear 512, pseudogene	-3
		GATSL2	GATS protein-like 2	-3
		SNORD114-28	small nucleolar RNA, C/D box 114-28	-3
		LOC102724842	uncharacterized LOC102724842	-3
		RNU6-960P	RNA, U6 small nuclear 960, pseudogene	-3
		SNORD114-26	small nucleolar RNA, C/D box 114-26	-3
		KIF14	kinesin family member 14	-3
		CLSPN	claspin	-3
		NAIP	NLR family, apoptosis inhibitory protein	-3
		FAR2P1	fatty acyl CoA reductase 2 pseudogene 1	-3
		CTD-2306M5.1	novel transcript	-3
		ASPM	asp (abnormal spindle) homolog, microcephaly associated (Drosophila)	-3
		ELOVL2	ELOVL fatty acid elongase 2	-3
		HELLS	helicase, lymphoid-specific	-3
		HAPLN1	hyaluronan and proteoglycan link protein 1	-3
		RNU6-971P	RNA, U6 small nuclear 971, pseudogene	-3
		MELK	maternal embryonic leucine zipper kinase	-3
		LOC101929381	uncharacterized LOC101929381	-3

nPTB	2nd	Symbol	Title	Δ
		RN7SKP42	RNA, 7SK small nuclear pseudogene 42	-3
		PABPC4L	poly(A) binding protein, cytoplasmic 4-like	-3
		RNU6-623P	RNA, U6 small nuclear 623, pseudogene	-3
		POT1-AS1	POT1 antisense RNA 1	-3
		CDYL2	chromodomain protein, Y-like 2	-3
		RNU6-780P	RNA, U6 small nuclear 780, pseudogene	-3
		KAL1	Kallmann syndrome 1 sequence	-3
		ERBB3	v-erb-b2 avian erythroblastic leukemia viral oncogene homolog 3	-4
		ZNF283	zinc finger protein 283	-4
		FMOD	fibromodulin	-4
		LAMA2	laminin, alpha 2	-4
		PDIA5	protein disulfide isomerase family A, member 5	-4
		METTL7A	methyltransferase like 7A	-4
		CENPE	centromere protein E, 312kDa	-4
		F5	coagulation factor V (proaccelerin, labile factor)	-4
		ANKRD36BP2	ankyrin repeat domain 36B pseudogene 2	-4
		HNRNPA1P33	heterogeneous nuclear ribonucleoprotein A1 pseudogene 33	-4
		MEST	mesoderm specific transcript	-4
		CKAP2	cytoskeleton associated protein 2	-4
		KIF11	kinesin family member 11	-4
		DPT	dermatopontin	-4
		CASC5	cancer susceptibility candidate 5	-4
		MIR580	microRNA 580	-4
		VIT	vitrin	-4
		CENPH	centromere protein H	-4
		RNU6-1170P	RNA, U6 small nuclear 1170, pseudogene	-4
		SCARNA9L	small Cajal body-specific RNA 9-like	-4
		RNU6-77P	RNA, U6 small nuclear 77, pseudogene	-4
		RAD51	RAD51 recombinase	-4
		RNU6-375P	RNA, U6 small nuclear 375, pseudogene	-4
		MIR205HG	MIR205 host gene (non-protein coding)	-4
		RNU6-595P	RNA, U6 small nuclear 595, pseudogene	-4
		AC009262.2	putative novel transcript	-5
		RNU6-308P	RNA, U6 small nuclear 308, pseudogene	-5
		FGF7	fibroblast growth factor 7	-5
		BRIP1	BRCA1 interacting protein C-terminal helicase 1	-5
		RNU6-151P	RNA, U6 small nuclear 151, pseudogene	-5
		LRP2	low density lipoprotein receptor-related protein 2	-5
		TSPAN2	tetraspanin 2	-5
		NPPB	natriuretic peptide B	-5
		HIST1H3B	histone cluster 1, H3b	-5
		RNU2-63P	RNA, U2 small nuclear 63, pseudogene	-5
		RNU6-560P	RNA, U6 small nuclear 560, pseudogene	-6
		COL1A2	collagen, type I, alpha 2	-6
		MIR515-1	microRNA 515-1	-6
		COL3A1	collagen, type III, alpha 1	-6
		PRSS12	protease, serine, 12 (neurotrypsin, motopsin)	-6
		HGF	hepatocyte growth factor (hepapoietin A; scatter factor)	-7
		RNU6-606P	RNA, U6 small nuclear 606, pseudogene	-7
		RP11-308B16.2	putative novel transcript	-7

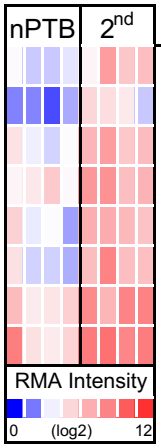

Symbol	Title	Δ
RNU2-29P	RNA, U2 small nuclear 29, pseudogene	-7
RNU6-989P	RNA, U6 small nuclear 989, pseudogene	-7
LOC389765	kinesin family member 27 pseudogene	-8
CGA	glycoprotein hormones, alpha polypeptide	-8
PDIA3P1	protein disulfide isomerase family A, member 3 pseudogene 1	-8
RNU6-79P	RNA, U6 small nuclear 79, pseudogene	-10
HIST1H2AM	histone cluster 1, H2am	-11
RP11-318G21.4	putative novel transcript	-17

Supplemental Figure 5. Global gene expression profiles of schCTBs isolated by laser capture microdissection from the fetal membranes: non infected preterm birth (nPTB) as compared to the late second trimester of normal pregnancy (2^{nd}) (n=4/group). The heatmap lists genes that were differentially expressed by 2-fold or greater.

Table S1. Maternal and neonatal characteristics (morphology, immunolocalization, invasion and proliferation experiments).

	sPE (n=7)*	nPTB (n=5)*	P value**
Maternal age (years)	27.86 (2.94)	30.20 (2.22)	> 0.05
BMI, Kg/m^2	29.90 (2.12)	24.06 (1.19)	> 0.05
Systolic blood pressure, mmHg	150.5 (6.58)	116.5 (4.34)	< 0.01
Diastolic blood pressure, mmHg	88 (3.56)	68.2 (3.86)	< 0.01
Preoteinuria	+1 to +3	0 or NA	< 0.05
Gestational age at delivery (week)	30.93 (1.42)	32.87 (0.66)	> 0.05
Birth weight, g	1264.29 (307.02)	1957.6 (154.19)	< 0.05

* mean ± SD

** 2-tailed Student´s t-test

NA: Not available

Table S2. Maternal and neonatal characteristics (transcriptional profiling).

	sPE (n=4)*	nPTB (n=4)*	P value**
Maternal age (years)	29.0 (3.34)	31.7 (2.3)	> 0.05
BMI, Kg/m^2	29.95 (3.59)	25.0 (1.89)	> 0.05
Systolic blood pressure, mmHg	152.0 (6.58)	117.8 (7.82)	< 0.02
Diastolic blood pressure, mmHg	91.62 (3.25)	72.7 (4.97)	< 0.02
Proteinuria	+1 to +3	0 or NA	< 0.05
Gestational age at delivery (weeks)	26.0 (3.76)	32.4 (0.82)	> 0.05
Birth weight (grams)	908.75 (177.82)	2083.3 (207.87)	< 0.01

* mean ± SD

** 2-tailed Student´s t-test

NA: Not available

Table S3. Antibodies

Antibody	Catalog Number/ Clone	Source	Concentration (μg/ml)
Vimentin	V4630	Sigma Aldrich	72.6
CK7	7D3	Damsky et al., 1992*	26
HLA-G	4H84	McMaster et al., 1998**	20
ITGA4	NBP1-77333	Novus Biologicals	10
E-cadherin	36/E-cadherin	BD Biosciences	2.5
hPL	MCA331	Serotec	50
GSTA3	sc-100547	Santa Cruz Biotechnology	1
PAPP-A	ab203683	Abcam	10
anti-rabbit secondary Ab	A21206	Life Technologies	2
anti-goat secondary Ab	A11055	Life Technologies	2
anti-mouse secondary Ab	A21907	Life Technologies	2
anti-rat secondary Ab	712-025-153	Jackson ImmunoResearch	15

*Damsky C, et al 1992. Distribution patterns of extracellular matrix components and adhesion receptors are intricately modulated during first trimester cytotrophoblast differentiatin along the invasive pathway, in vivo. J Clin Invest. 89: 210-22

**McMaster M, et al 1998. HLA-G isoforms produced by lplacental cytrotrophoblasts and found in amniotic fluid are due to unusual glycosylation. J Immunol. 160(12) 5922-8.